

A Resonance-free Adaptive Levin Method in Two-Dimensions

Murdock Aubry¹ Kirill Serkh^{1,2} James Bremer²

¹Department of Computer Science, University of Toronto

²Department of Mathematics, University of Toronto

Abstract

Oscillatory integrals are often handled by the classical Levin method which operates by solving a particular differential equation for the antiderivative of the integrand. Recent works have displayed that, although long believed to have suffered from low-frequency breakdown; the Levin method can rapidly produce accurate solutions for all orders frequency if deployed properly. Recent experimental evidence, shortly followed by theoretical proof, has shown that if Chebyshev spectral methods are used to discretize the aforementioned differential equation and then the resulting linear system is solved via a truncated singular value decomposition, then no low-frequency breakdown occurs.

In this paper, we generalize the previous algorithms and theoretical results from the one-dimensional Levin method in order to evaluate integrals over two-dimensional domains. We provide two variants of this generalization with distinct assumptions on the functions involved. Each of these variants operates by solving a differential equation for the anti-divergence of the integrand. Under particular assumptions, the resulting differential equation admits a slowly varying vector field solution, allowing the boundary integral to be rapidly evaluated using one-dimensional Levin algorithm. We describe a method of obviating the resonance problem by forcing alignment in vector field the solution with direction of maximal normed frequency, ensuring maximal frequency along the boundary integral. We provide proof that when the integrand is either slowly oscillating or even contains stationary points, the algorithm does not suffer from low frequency breakdown. Extensive experiments testing these algorithms is reported for a vast class of oscillatory integrals. The results highlight the high performance, efficiency and robustness of these algorithms, further showing that in absence of low-frequency breakdown, the two-dimensional Levin method is suitable for use as the basis of an adaptive scheme.

1 Introduction

First introduced by David Levin in [4], the Levin method is a classical technique for evaluating one-dimensional integrals of the form

$$\int_a^b f(x) \exp(ig(x)) dx, \quad (1)$$

where $f : \mathbb{R} \rightarrow \mathbb{C}$ is a slowly varying, possibly complex valued function, $g : \mathbb{R} \rightarrow \mathbb{R}$ a slowly varying scalar valued function, g' is of large magnitude.

It operates by solving the first order ordinary differential equation

$$p'(x) + ig'(x)p(x) = f(x) \quad (2)$$

which, under the above assumptions, admits and slowly varying solution $p(x)$ such that

$$\frac{d}{dx} (p(x) \exp(ig(x))) = f(x) \exp(ig(x)). \quad (3)$$

The value of (1) is then given by

$$p(b) \exp(ig(b)) - p(a) \exp(ig(a)). \quad (4)$$

Recent work [5],[6] presents experimental evidence that if Chebyshev spectral methods are used to discretize (2), and a truncated singular value decomposition is used to solve the system, then no frequency breakdown occurs. Following this, [3] proved this to be the case, regardless of the magnitude or number of stationary points of g . Since g' need not be invertible, they further prove that the Levin equation admits a solution that can be approximated by a polynomial expansion at a cost which decreases with the magnitude of g' . Finally, they implement an adaptive algorithm and provide vast experimental results displaying the accuracy and robustness of this method.

In this paper, we generalize the adaptive scheme discussed in [3] to handle two dimensional integrals over a rectangle $R \subset \mathbb{R}^2$. Specifically, we handle integrals of the form

$$I = \int_R f(x, y) \exp(ig(x, y)) dx dy, \quad (5)$$

where

- $R = [a, b] \times [c, d]$ a rectangle in the plane,
- $f : \mathbb{R}^2 \rightarrow \mathbb{C}$ a scalar function on the plane and
- $g : \mathbb{R}^2 \rightarrow \mathbb{R}$ a scalar function on the plane, slowly varying, and ∇g is of large magnitude.

The algorithm operates by solving the partial differential equation

$$\nabla \cdot \mathbf{p}(x, y) + i\nabla g(x, y) \cdot \mathbf{p}(x, y) = f(x, y), \quad (6)$$

where $\nabla g(x, y)$ is the gradient of the function g . Then the vector-valued solution $\mathbf{p}(x, y) = \begin{pmatrix} p_1(x, y) \\ p_2(x, y) \end{pmatrix}$ to (6) satisfies

$$\nabla \cdot (\mathbf{p}(x, y) \exp(ig(x, y))) = f(x, y) \exp(ig(x, y)). \quad (7)$$

Substituting this into integral (5) and applying the divergence theorem, we obtain the integral

$$I = \int_{\partial R} \mathbf{p}(x, y) \exp(ig(x, y)) d\ell(x, y) \quad (8)$$

which can be written as

$$\begin{aligned} I = & - \int_a^b p_2(x, c) \exp(ig(x, c)) dx + \int_c^d p_1(b, y) \exp(ig(b, y)) dy \\ & + \int_a^b p_2(x, d) \exp(ig(x, d)) dx - \int_c^d p_1(a, y) \exp(ig(a, y)) dy \end{aligned} \quad (9)$$

Similar to the one-dimensional case, the differential operator

$$\mathbf{L}[\mathbf{p}](x, y) = \nabla \cdot \mathbf{p}(x) + i\nabla g(x, y) \cdot \mathbf{p}(x, y) \quad (10)$$

has a nullspace consisting of vector fields of the form

$$\mathbf{p}(x, y) = \mathbf{q}(x, y) \exp(-ig(x, y)) \quad (11)$$

where \mathbf{q} is divergenceless; $\nabla \cdot \mathbf{q}(x, y) = 0$.

In this work, we prove that when bivariate Chebyshev spectral methods are used to discretize (6), and the resulting linear system is solved via a truncated singular value decomposition, no low frequency breakdown occurs.

First, we prove that when ∇g is non-vanishing, the two-dimensional Levin equations admit well-behaved solutions that can be approximated by bivariate polynomial expansions. We then consider the case where ∇g is of small magnitude and possibly has zeroes, in which case ∇g is not invertible. We show that even in this case, the two-dimensional Levin method admits a well-behaved solution. These results generalizes the results of [3].

Note that the proofs of these results are negligibly dependent on the dimension of the ambient space. All theorems and results can be trivially modified to obtain analogous results for the case where $f, g : \mathbb{R}^n \rightarrow \mathbb{R}$ for any value of n . In this report, however, we exclusively present results pertaining to the case where $n = 2$.

2 Preliminaries

2.1 Notation and Conventions

The use of capital scripted letters of the form \mathcal{A} are reserved for matrices, and bold letters \mathbf{v} reserved to denote vectors. We denote by $\text{diag}(\mathbf{v})$, for a vector \mathbf{v} of length n , the $n \times n$ diagonal matrix with diagonal entries being the components of \mathbf{v} :

$$\text{diag}(\mathbf{v}) = \begin{pmatrix} v_1 & & \\ & \ddots & \\ & & v_n \end{pmatrix}. \quad (12)$$

Similarly, we denote by $\text{diag}_n(\lambda)$ for some constant λ the $n \times n$ diagonal matrix with diagonal entries uniformly λ :

$$\text{diag}_n(\lambda) = \begin{pmatrix} \lambda & & \\ & \ddots & \\ & & \lambda \end{pmatrix}. \quad (13)$$

We denote by $B_r(a, b)$ the closed ball of radius r centred at the point $(a, b) \in \mathbb{R}^2$. That is,

$$B_r(a, b) = \{(x, y) \in \mathbb{R}^2 : (x - a)^2 + (y - b)^2 \leq r^2\} \quad (14)$$

We write $C^n([a, b])$ to denote the set of functions whose derivatives of orders up to or less than n are uniformly continuous on the interval $[a, b]$. In the case where $n = \infty$, $C^\infty([a, b])$ denotes the set of infinitely differentiable functions whose derivatives are uniformly continuous on the interval $[a, b]$. We extend this notation to handle multi-indices of the form $f(x, y) \in C^{(n,m)}(R)$ for some $R \subset \mathbb{R}^2$ to denote the fact that f is C^n in x and C^m in y for $(x, y) \in R$.

We denote by $S(\mathbb{R}^n, \mathbb{R}^m)$ the Schwartz space of infinitely differentiable functions $f : \mathbb{R}^n \rightarrow \mathbb{R}^m$ whose derivatives of all orders decay faster than any polynomial, while reserving $S(\mathbb{R}^n)$ for the case where $m = 1$.

The space of tempered distributions is denoted by $S'(\mathbb{R}^n)$. For $f \in S(\mathbb{R}^n)$ and tempered distributions $\varphi \in S'(\mathbb{R}^n)$, we write $\langle \varphi, f \rangle$ to denote the action of φ on f , given by the formula

$$\langle \varphi, f \rangle = \int_{\mathbb{R}^2} \varphi(x, y) f(x, y) dx dy. \quad (15)$$

The order of a tempered distribution $\varphi \in S(\mathbb{R})$ is the least non-negative integer N such that for all compact sets $K \subset \mathbb{R}$, there exists a constant M_K such that

$$|\langle \varphi, f \rangle| \leq M_K \sup_{0 \leq k \leq N} \sup_{x \in K} |D^k f(x)| \quad (16)$$

for all $f \in S(\mathbb{R})$ with $\text{supp}(f) \subset K$. Further, we introduce the double-index notation (N_1, N_2) to denote the order of a tempered distribution $\varphi \in S'(\mathbb{R}^2)$ which is of order N_1 in the first variable and of order N_2 in the second variable. Explicitly, for all compact $K \subset \mathbb{R}^2$ there exists a constant M_K such that

$$|\langle \varphi, f \rangle| \leq M_K \sup_{0 \leq k \leq N_1} \sup_{(x,y) \in K} |D_x^k f(x, y)| \quad |\langle \varphi, f \rangle| \leq M_K \sup_{0 \leq k \leq N_2} \sup_{(x,y) \in K} |D_y^k f(x, y)| \quad (17)$$

for every $f \in S(\mathbb{R}^2)$ with $\text{supp}(f) \subset K$.

For a function $f \in S(\mathbb{R}^2)$, we use the convention

$$\hat{f}(\xi, y) = \frac{1}{2\pi} \int_{-\infty}^{\infty} f(x, y) \exp(-i\xi x) dx \quad (18)$$

for the Fourier transform of f in the variable x , and

$$\hat{f}(x, y) = \int_{-\infty}^{\infty} f(\xi, y) \exp(i\xi x) d\xi \quad (19)$$

the inverse Fourier transform. Formulas are given analogously for the Fourier transform in y . By extension, we

utilize

$$\hat{f}(\xi_1, \xi_2) = \frac{1}{4\pi^2} \int_{\mathbb{R}^2} f(x, y) \exp(-i(\xi_1 x + \xi_2 y)) dx dy \quad (20)$$

for the Fourier transform of f in both variables, and

$$f(x, y) = \int_{\mathbb{R}^2} \hat{f}(\xi_1, \xi_2) \exp(i(\xi_1 x + \xi_2 y)) d\xi_1 d\xi_2 \quad (21)$$

the inverse Fourier transform of \hat{f} in both variables.

Throughout, we utilize the notation $x \lesssim y$ to indicate there is some constant C independent of y such that $x \leq Cy$. We say that

$$f(x, y) = \mathcal{O}(g(x, y)) \text{ as } \|(x, y)\| \rightarrow \infty \quad (22)$$

if there exists constants M and C such that

2.2 Bivariate Chebyshev expansions

We denote by $T_n(x)$ the Chebyshev polynomial of degree n , and

$$-1 = x_{1,k}^{\text{cheb}} < x_{2,k}^{\text{cheb}} < \dots < x_{k,k}^{\text{cheb}} = 1 \quad (23)$$

the k -point grid of Chebyshev extremal nodes which are given by

$$x_{j,k}^{\text{cheb}} = \cos\left(\pi \frac{k-j}{k-1}\right), \quad j = 1, \dots, k. \quad (24)$$

For the square $R = [-1, 1]^2$, denote by

$$\{x_{i,k}^{\text{cheb}}, x_{j,k}^{\text{cheb}}\}_{i,j=1}^k \quad (25)$$

the $k \times k$ tensor product Chebyshev extremal grid on R , where $\{x_{i,k}^{\text{cheb}}\}_{i=1}^k$ is the the k -point grid of Chebyshev extremal nodes on the interval $[-1, 1]$. This extremal grid can be mapped to any rectangle $[a, b] \times [c, d] \subset \mathbb{R}^2$ via the affine bilinear mapping

$$\mathbf{L}(x, y) = \left(\frac{b-a}{2}x + \frac{b+a}{2}, \frac{d-c}{2}y + \frac{d+c}{2} \right). \quad (26)$$

For functions $f \in C^\infty(R, \mathbb{C})$, we define $P_n[f]$ to be the bivariate Chebyshev series

$$P_n[f] = \sum_{0 \leq i+j < n} a_{ij} T_i(x) T_j(y). \quad (27)$$

which interpolates f at the nodes of the $k \times k$ -point Chebyshev tensor product extremal grid. If $f \in C^\infty(R, \mathbb{C})$, then it admits a uniformly convergent Chebyshev expansion

$$f(x, y) = \sum_{i,j=0}^{\infty} b_{ij} T_i(x) T_j(y). \quad (28)$$

It is well known that $P_n[f]$ converges to f faster than any polynomial. In particular,

$$|b_{ij}| = \mathcal{O}\left(\frac{1}{i^l j^k}\right) \quad (29)$$

for all $l, k \geq 1$. Resultingly, for all $0 < \epsilon < 1$, we can choose n sufficiently large such that

$$\|P_n[f] - f\|_{L^\infty(R)} \leq \epsilon \|f\|_{L^\infty(R)} \quad \text{and} \quad \left\| \frac{\partial}{\partial x} P_n[f] - \frac{\partial}{\partial x} f \right\| \leq \epsilon \|f\|_{L^\infty(R)}. \quad (30)$$

By extension, it follows that

$$\|P_n[f]\|_{L^\infty(R)} \leq 2\|f\|_{L^\infty(R)} \quad \text{and} \quad \left\| \frac{\partial}{\partial x} P_n[f] \right\|_{L^\infty(R)} \leq 2 \left\| \frac{\partial f}{\partial x} \right\|_{L^\infty(R)}. \quad (31)$$

Moreover, for any two functions $f, g \in C^\infty(R)$, we have the following inequality;

$$\|P_n[f]P_n[g] - fg\|_{L^\infty(R)} \leq \|P_n[f]\|_{L^\infty(R)}\|P_n[g] - g\|_{L^\infty(R)} + \|P_n[g]\|_{L^\infty(R)}\|P_n[f] - f\|_{L^\infty(R)} \quad (32)$$

$$\leq 4\epsilon\|f\|_{L^\infty(R)}\|g\|_{L^\infty(R)} \quad (33)$$

We utilize the notation $[f]$ to denote the vector

$$[f] = \begin{pmatrix} f(x_{1,k}^{\text{cheb}}, y_{1,k}^{\text{cheb}}) \\ f(x_{2,k}^{\text{cheb}}, y_{1,k}^{\text{cheb}}) \\ \vdots \\ f(x_{k,k}^{\text{cheb}}, y_{1,k}^{\text{cheb}}) \\ f(x_{1,k}^{\text{cheb}}, y_{2,k}^{\text{cheb}}) \\ f(x_{2,k}^{\text{cheb}}, y_{2,k}^{\text{cheb}}) \\ \vdots \\ f(x_{k,k}^{\text{cheb}}, y_{k,k}^{\text{cheb}}) \end{pmatrix} \quad (34)$$

of values of an expansion of the form $P_n[f]$ at the tensor product extremal Chebyshev nodes on the rectangle R . We represent the vector field $F : \mathbb{R}^2 \rightarrow \mathbb{R}^2$, where

$$\mathbf{F}(x, y) = \begin{pmatrix} F_1(x, y) \\ F_2(x, y) \end{pmatrix} \quad (35)$$

via the concatenated vector

$$[\mathbf{F}] = \begin{pmatrix} [F_1] \\ [F_2] \end{pmatrix}. \quad (36)$$

The k^{th} order bivariate Chebyshev partial spectral differentiation matrices are the $k^2 \times k^2$ matrices \mathcal{D}_x^k and \mathcal{D}_y^k which maps the vector $[f]$ to the vectors

$$\left[\frac{\partial f}{\partial x} \right] = \begin{pmatrix} \frac{\partial f}{\partial x}(x_{1,k}^{\text{cheb}}, y_{1,k}^{\text{cheb}}) \\ \frac{\partial f}{\partial x}(x_{2,k}^{\text{cheb}}, y_{1,k}^{\text{cheb}}) \\ \vdots \\ \frac{\partial f}{\partial x}(x_{k,k}^{\text{cheb}}, y_{1,k}^{\text{cheb}}) \\ \frac{\partial f}{\partial x}(x_{1,k}^{\text{cheb}}, y_{2,k}^{\text{cheb}}) \\ \frac{\partial f}{\partial x}(x_{2,k}^{\text{cheb}}, y_{2,k}^{\text{cheb}}) \\ \vdots \\ \frac{\partial f}{\partial x}(x_{k,k}^{\text{cheb}}, y_{2,k}^{\text{cheb}}) \end{pmatrix} \quad \left[\frac{\partial f}{\partial y} \right] = \begin{pmatrix} \frac{\partial f}{\partial y}(x_{1,k}^{\text{cheb}}, y_{1,k}^{\text{cheb}}) \\ \frac{\partial f}{\partial y}(x_{2,k}^{\text{cheb}}, y_{1,k}^{\text{cheb}}) \\ \vdots \\ \frac{\partial f}{\partial y}(x_{k,k}^{\text{cheb}}, y_{1,k}^{\text{cheb}}) \\ \frac{\partial f}{\partial y}(x_{1,k}^{\text{cheb}}, y_{2,k}^{\text{cheb}}) \\ \frac{\partial f}{\partial y}(x_{2,k}^{\text{cheb}}, y_{2,k}^{\text{cheb}}) \\ \vdots \\ \frac{\partial f}{\partial y}(x_{k,k}^{\text{cheb}}, y_{2,k}^{\text{cheb}}) \end{pmatrix} \quad (37)$$

of values of the partial derivatives of f at the tensor product Chebyshev extremal grid. That is,

$$\mathcal{D}_x^k[f] = \left[\frac{\partial f}{\partial x} \right] \quad \mathcal{D}_y^k[f] = \left[\frac{\partial f}{\partial y} \right]. \quad (38)$$

2.3 Truncated singular value decomposition

If \mathcal{A} is an complex-valued $n \times m$ matrix where $n \leq m$, then any decomposition of the form

$$\mathcal{A} = \begin{pmatrix} | & & | \\ \mathbf{u}_1 & \cdots & \mathbf{u}_n \\ | & & | \end{pmatrix} \begin{pmatrix} \sigma_1 & & \\ & \ddots & \\ & & \sigma_n \end{pmatrix} \begin{pmatrix} | & & | \\ \mathbf{v}_1 & \cdots & \mathbf{v}_m \\ | & & | \end{pmatrix}^T, \quad (39)$$

is referred to as a singular value decomposition of \mathcal{A} . Here, $\sigma_1, \dots, \sigma_n \in \mathbb{R}$ are singular values, and $\{\mathbf{u}_1, \dots, \mathbf{u}_n\}$ and $\{\mathbf{v}_1, \dots, \mathbf{v}_m\}$ are the left and right singular vectors which form orthonormal bases of \mathbb{C}^n and \mathbb{C}^m respectively. The quantities $\{\sigma_i\}_{i=1}^n$ are referred to as the singular values. They are unique up to ordering, and are conventionally ordered in descending order.

A *truncated* singular value decomposition of the matrix \mathcal{A} is any approximation of the form

$$\mathcal{A} = \begin{pmatrix} | & & | \\ \mathbf{u}_1 & \cdots & \mathbf{u}_k \\ | & & | \end{pmatrix} \begin{pmatrix} \sigma_1 & & \\ & \ddots & \\ & & \sigma_k \end{pmatrix} \begin{pmatrix} | & & | \\ \mathbf{v}_1 & \cdots & \mathbf{v}_k \\ | & & | \end{pmatrix}^T, \quad (40)$$

where $1 \leq k \leq n$, and each $\mathbf{u}_i \in \mathbb{C}^n$ and $\mathbf{v}_i \in \mathbb{C}^m$. An algorithm which computes the truncated singular value decomposition takes as input some desired precision parameter $\epsilon > 0$. The truncation integer k is then taken to be the smallest integer between 1 and $n - 1$ such that $\sigma_k < \epsilon$, or $k = n$ otherwise. The approximate solution $\tilde{\mathbf{x}}$ to the linear system $\mathcal{A}\mathbf{x} = \mathbf{y}$ is then taken to be

$$\tilde{\mathbf{x}} = \begin{pmatrix} | & & | \\ \mathbf{v}_1 & \cdots & \mathbf{v}_k \\ | & & | \end{pmatrix} \begin{pmatrix} \frac{1}{\sigma_1} & & \\ & \ddots & \\ & & \frac{1}{\sigma_k} \end{pmatrix} \begin{pmatrix} | & & | \\ \mathbf{u}_1 & \cdots & \mathbf{u}_k \\ | & & | \end{pmatrix}^T \mathbf{y}. \quad (41)$$

The following lemma is a simplified version of Theorem 2.1 in [7].

Lemma 1. Suppose that $\epsilon > 0$, and \mathcal{A} is an $n \times n$ matrix with complex entires. Further, suppose

$$\mathcal{A}\mathbf{x} = \mathbf{y} + \delta\mathbf{y} \quad (42)$$

for some \mathbf{x}, \mathbf{y} and $\delta\mathbf{y} \in \mathbb{C}^n$ with

$$\|\delta\mathbf{y}\| \lesssim \epsilon \|\mathcal{A}\| \|\mathbf{x}\|. \quad (43)$$

Suppose further that the linear system

$$\mathcal{A}\mathbf{x} = \mathbf{y} \quad (44)$$

is solved in finite precision arithmetic using a singular value decomposition which is truncated at precision $\epsilon \|\mathcal{A}\|$, and that \mathbf{z} is the resulting solution. Then

$$\|\mathbf{z}\| \lesssim \|\mathbf{x}\| \quad (45)$$

and

$$\|\mathcal{A}\mathbf{z} - \mathbf{y}\| \lesssim \epsilon \|\mathcal{A}\| \|\mathbf{x}\|. \quad (46)$$

The above lemma implies that when a linear system admits an approximate solution with a modest norm, a truncated singular value decomposition can be used to obtain a solution with both a small residual and modest norm.

2.4 Approximation by bandlimited functions

Throughout the analysis of the two-dimensional Levin equation, it will often be necessary to approximate a function $f : R \rightarrow \mathbb{R}$, where $R = [-1, 1]^2$, via a well behaved bandlimited function f_b on an open neighbourhood of the domain of f . In this report, we take the term 'well-behaved' to mean that the $L^\infty(\mathbb{R}^2)$ norms of f_b , \hat{f}_b and the derivatives of \hat{f}_b are bounded by small constant multiples of the $L^\infty(R)$ norm of f . To ensure a tight bound on the approximation f_b , it is often desirable to choose the minimal bandlimit subject to the above constraints.

The existence of such a bandlimited function f_b of f is provable under certain regularity conditions on f . The following theorem is a dimensional generalization of Theorem 1 in [3], which itself is a slightly modified version of Theorem 1 of [1]. The relatively weak conditions on f of this theorem is an example of sufficient regularity to ensure existence of such a bandlimit f_b .

Theorem 1. *Suppose that $f : R \rightarrow \mathbb{C}$ admits an infinitely differentiable extension to an open neighbourhood of R . Then for each positive integer m and each real number $c > 1$, there exists a constant $k(m)$ independent of c , and a function $f_b \in S(\mathbb{R}^2)$ such that*

1. \hat{f}_b is supported on $[-c - 2, c + 2]^2$,
2. $\|f_b - f\|_{L^\infty(R)} < \frac{k(m)}{c^m}$,
3. $\|f_b\|_{L^\infty(\mathbb{R}^2)} \leq 2\|f\|_{L^\infty(R)} + \frac{k(m)}{c^m}$,
4. $\|\hat{f}_b\|_{L^\infty(\mathbb{R}^2)} \leq \|f\|_{L^\infty(R)}$ and
5. $\left\| \frac{\partial}{\partial \xi_i} \hat{f}_b \right\|_{L^\infty(\mathbb{R}^2)} \leq 2\|f\|_{L^\infty(R)}$ for $i = 1, 2$.

Proof. Here, for simplicity, we prove the existence of such a bandlimited function in the case where $f : B_1(0, 0)$. Of course, composing with a diffeomorphism $\mathbf{F} : R \rightarrow B_1(0, 0)$ which admits a diffeomorphic extension to an open neighbourhood of R , we obtain the results of Theorem (1). Explicitly, if $f : R \rightarrow \mathbb{C}$ admits an infinitely differentiable extension to an open neighbourhood of R , then $f \circ \mathbf{F}^{-1} : B_r(0, 0) \rightarrow \mathbb{C}$ admits an infinitely differentiable extension to an open neighbourhood of $B_r(0, 0)$. An example of such a diffeomorphism could be given by

$$\mathbf{F}(x, y) = \begin{pmatrix} x\sqrt{1 - \frac{y^2}{2}} & y\sqrt{1 - \frac{x^2}{2}} \\ \sqrt{1 - \frac{x^2 y^2}{4}} & \sqrt{1 - \frac{x^2 y^2}{4}} \end{pmatrix}. \quad (47)$$

We begin by defining $M = \|f\|_{L^\infty(B_1(0,0))}$ and let $0 < \delta < 1$ be so small such that

$$\|f\|_{L^\infty(B_{1+\delta}(0,0))} \leq 2M. \quad (48)$$

Moreover, we define a window function $T_1(x, y) \in C^\infty(\mathbb{R}^2)$ such that $T_1(x, y) = 1$

$$T_1(x, y) = \begin{cases} 1, & r \leq 1, \\ 0, & r > 1 + \delta, \end{cases} \quad (49)$$

where $r = \sqrt{x^2 + y^2}$ and $|T(x, y)| \leq 1$ for all $(x, y) \in \mathbb{R}^2$. An example of such a function is

$$T_1(x, y) = \begin{cases} 1, & r \leq 1, \\ H\left(\frac{\delta-1}{\delta} - \frac{r}{\delta}\right), & 1 < r \leq 1 + \delta, \\ 0, & r > 1 + \delta. \end{cases} \quad (50)$$

where $H(x)$ is the infinitely differentiable ramp function

$$H(x) = \begin{cases} \frac{1}{2} \left(1 + \operatorname{erf}\left(\frac{x}{\sqrt{1-x^2}}\right) \right), & |x| \leq 1, \\ 0, & |x| > 1. \end{cases} \quad (51)$$

Now consider $f_1(x, y) = f(x, y)T_1(x, y)$. Since $f \in S(\mathbb{R}^2)$ and T_1 is infinitely differentiable, it follows that both $f_1, \hat{f}_1 \in S(\mathbb{R}^2)$. Therefore, \hat{f}_1 is rapidly decaying, providing us with the following inequality;

$$\sup_{|\xi| \geq 1} |\hat{f}_1(\xi_1, \xi_2)| \leq \frac{k_1(m)}{|\xi|^{m+2}}, \quad (52)$$

where $\xi = (\xi_1, \xi_2)$. Since $|T_1(x, y)| \leq 1$, it follows that $|f_1(x, y)| \leq 2M$ for all $(x, y) \in R$. We compute

$$\left| \hat{f}_1(\xi_1, \xi_2) \right| = \left| \frac{1}{4\pi^2} \int_{B_{1+\delta}(0,0)} f_1(x, y) \exp(-i(\xi_1 x + \xi_2 y)) dx dy \right| \quad (53)$$

$$\leq \frac{1}{4\pi^2} 2M(1 + \delta)^2 \pi \quad (54)$$

$$\leq \frac{2M}{\pi}. \quad (55)$$

Similarly,

$$\left| \frac{d}{d\xi_1} \hat{f}_1(\xi_1, \xi_2) \right| = \left| \frac{-i}{4\pi^2} \int_{B_{1+\delta}(0,0)} f_1(x, y) x \exp(-i(\xi_1 x + \xi_2 y)) dx dy \right| \leq \frac{4M}{\pi}, \quad (56)$$

$$\left| \frac{d}{d\xi_2} \hat{f}_1(\xi_1, \xi_2) \right| = \left| \frac{-i}{4\pi^2} \int_{B_{1+\delta}(0,0)} f_1(x, y) y \exp(-i(\xi_1 x + \xi_2 y)) dx dy \right| \leq \frac{4M}{\pi}. \quad (57)$$

We now define a second windowing function $T_2 \in C^\infty(\mathbb{R}^2)$ such that

1. $|T_2(x, y)| \leq 1$ for all $(x, y) \in \mathbb{R}^2$,
2. $\left| \frac{d}{dx} T_2(x, y) \right| \leq 1$ and $\left| \frac{d}{dy} T_2(x, y) \right| \leq 1$ for all $(x, y) \in \mathbb{R}^2$,
3. $T_2(x, y) = 1$ for all $r \leq c$ and
4. $T_2(x, y) = 0$ for all $r > c + 1$.

Once again, an example of such a function can be constructed by utilizing the ramp function discussed above. Explicitly, take

$$T_2(x, y) = \begin{cases} 1, & r \leq 1, \\ H\left(\frac{c-1}{c} - \frac{r}{c}\right), & 1 < r \leq 1 + c, \\ 0, & r > 1 + c. \end{cases} \quad (58)$$

Since $c > 1$, it follows that property 2 of T_2 holds. Now, by defining

$$\hat{f}_b(\xi_1, \xi_2) = \hat{f}_1(\xi_1, \xi_2) T_2(\xi_1, \xi_2), \quad (59)$$

property 1 is immediately satisfied. Recalling the inequality (52) and that $|T_2(x, y)| \leq 1$, it follows that

$$|f_1(x, y) - f_b(x, y)| = \left| \frac{1}{4\pi^2} \int_{\mathbb{R}^2} \hat{f}_1(\xi_1, \xi_2) (1 - T_2(\xi_1, \xi_2)) \exp(i(\xi_1 x + \xi_2 y)) d\xi_1 d\xi_2 \right| \quad (60)$$

$$\leq \frac{1}{2\pi^2} \int_{|\xi|>c} \left| \hat{f}_1(\xi_1, \xi_2) \right| d\xi_1 d\xi_2 \quad (61)$$

$$\leq \frac{1}{2\pi^2} \int_{|\xi|>c} \frac{k_1(m)}{|\xi|^{m+2}} d\xi_1 d\xi_2 \quad (62)$$

$$= \frac{1}{2\pi^2} \int_{r>c} \frac{k_1(m)}{r^{m+2}} r \cos^2 \theta dr d\theta \quad (63)$$

$$= \frac{k_1(m)}{2\pi m c^m}. \quad (64)$$

If we let $k(m) = \frac{k_1(m)}{2\pi m}$, conclusion 2 of the theorem follows immediately. Combining the above with the fact that

$|f_1(x, y)| \leq 2M$, we obtain property 3. Finally,

$$\left| \hat{f}_b(\xi_1, \xi_2) \right| = \left| \hat{f}_1(\xi_1, \xi_2) T_2(\xi_1, \xi_2) \right| \leq \frac{2M}{\pi}, \quad (65)$$

$$\left| \frac{\partial}{\partial \xi_i} \hat{f}_b(\xi_1, \xi_2) \right| = \left| \frac{\partial}{\partial \xi_i} \hat{f}_1(\xi_1, \xi_2) T_2(\xi_1, \xi_2) + \hat{f}_1(\xi_1, xi_2) \frac{\partial}{\partial \xi_i} T_2(\xi_1, \xi_2) \right| \leq \frac{2M}{\pi} + \frac{4M}{\pi} = \frac{6M}{\pi} \quad (66)$$

for $i = 1, 2$ establishes properties 4 and 5 of f_b above. \square

Definition 1. Suppose that $f : R \rightarrow \mathbb{C}$ admits an infinitely differentiable extension to an open neighbourhood of R . Then for each $0 < \epsilon < 1$, we denote by $c_f(\epsilon)$ the smallest positive real number c such that there exists a function $f_b \in S(\mathbb{R}^2)$ of bandlimit c such that

1. $\|f_b - f\|_{L^\infty(R)} < \epsilon \|f\|_{L^\infty(R)}$,
2. $\|f_b\|_{L^\infty(\mathbb{R}^2)} \leq 4\|f\|_{L^\infty(R)}$,
3. $\|\hat{f}_b\|_{L^\infty(\mathbb{R}^2)} \leq \|f\|_{L^\infty(R)}$ and
4. $\left\| \frac{\partial}{\partial \xi_i} \hat{f}_b \right\|_{L^\infty(\mathbb{R}^2)} \leq 2\|f\|_{L^\infty(R)}$ for $i = 1, 2$.

Of course, the existence of such a bandlimited function f_b of the function $f : R \rightarrow \mathbb{C}$ with associated bandlimit $c_f(\epsilon)$ is provided by Theorem (1).

The following result is an immediate consequence of Theorem (1).

Corollary 1. If $f : R \rightarrow \mathbb{R}$ admits an infinitely differentiable extension to a neighbourhood of R , then for every positive integer m ,

$$c_f(\epsilon) = \mathcal{O}\left(\left(\frac{1}{\epsilon}\right)^{\frac{1}{m}}\right) \text{ as } \epsilon \rightarrow 0. \quad (67)$$

2.5 Bivariate Legendre expansions of bandlimited functions

Throughout this subsection, we use the notation $P_k(x)$ to denote the Legendre polynomial of degree k . Moreover, we let $R = [-1, 1]^2$.

Lemma 2. If φ is a tempered distribution of order $(N, 0)$ which has support contained in some rectangle $R = [-c, c]^2$ for $c > 0$, then there exist one dimensional complex Radon measures $\{\nu_k\}_{k=0}^{N-1}$ on $[-c, c]$ and a complex Radon measure μ on R such that

$$\langle \varphi, f \rangle = \sum_{k=0}^{N-1} \int_{-c}^c \frac{\partial^k f}{\partial x^k}(0, y) d\nu_k(y) + \int_R \frac{\partial^N f}{\partial x^N}(x, y) d\mu(x, y) \quad (68)$$

for all $f(x, y) \in C^{(N,0)}(R)$.

Proof. Since the space of tempered distributions of order $(N, 0)$ which are supported on R can be identified as the dual space of $C^{(N,0)}(R)$, it suffices to show that any element of the dual of $C^{(N,0)}(R)$ is of the form (68). The case where $N = 0$ follows from a trivial application of the Riesz representation theorem, so suppose that $N \geq 1$. Define $h_k(y) : [-c, c] \rightarrow \mathbb{R}$ by

$$h_k(y) = \frac{\partial^k f}{\partial x^k}(0, y). \quad (69)$$

Since any function $f \in C^{(N,0)}(R)$ can be written as

$$f(x, y) = \sum_{k=0}^{N-1} h_k(y) \frac{x^k}{k!} + \frac{1}{(N-1)!} \int_0^x \frac{\partial^N f}{\partial x^N}(u, y) u^{N-1} du, \quad (70)$$

the map

$$f \mapsto \left(h_0(y), h_1(y), \dots, h_{N-1}(y), \frac{\partial^N f}{\partial x^N} \right) \quad (71)$$

is an isomorphism $C^{(N,0)}(R) \rightarrow \Pi_N(C^0[-c,c]) \times C(R)$ where $C(R)$ is the space of uniformly continuous functions on R . The result follows by observing that the dual of $C(R)$ is the space of complex Radon measures $M(R)$ and the dual of $C^0([-c,c])$ is the space of complex Radon measures $M([-c,c])$ \square

Lemma 3. *If the Fourier transform of a tempered distribution is of order $(N,0)$ and has support contained in a rectangle $R = [-c,c]^2$, then φ can be expressed as an entire function of the form*

$$\varphi(x,y) = \sum_{k=0}^{N-1} x^k \int_{-c}^c i^k \exp(iy\xi_2) d\nu_k(\xi_2) + x^N \int_R i^N \exp(i(\xi_1 x + \xi_2 y)) d\mu(\xi_1, \xi_2), \quad (72)$$

where $\mu \in M(R)$.

Proof. The tempered distribution φ is given by

$$\varphi(x,y) = \langle \hat{\varphi}, \xi_{(x,y)} \rangle \quad (73)$$

where

$$\xi_{(x,y)}(\xi_1, \xi_2) = \exp(i(\xi_1 x + \xi_2 y)) \quad (74)$$

Then the result follows immediately from Lemma (3). \square

The following Lemma is taken directly from [3], and is restated here for convenience.

Lemma 4. *For all real-valued ξ and non-negative integers k ,*

$$|\exp(i\xi x) P_k(x)| \leq \frac{2 \left| \frac{\xi}{2} \right|^k}{\Gamma(k+1)} \quad (75)$$

Theorem 2. *Suppose that the Fourier transform of $\varphi \in S'(\mathbb{R}^2)$ is a tempered distribution of order $(N,0)$ supported on $[-c,c]^2$ where $c \geq 1$. Then φ is an entire function and the coefficients of the Legendre expansion*

$$\varphi(x,y) = \sum_{l,m=0}^{\infty} a_{lm} P_l(x) P_m(y) \quad (76)$$

of φ satisfy

$$|a_{lm}| \lesssim \frac{\left(\frac{c}{2}\right)^{l+m+N}}{\Gamma(l-N+1)\Gamma(m+1)}. \quad (77)$$

for all $l \geq N$.

Proof. Let $R_c = [-c,c]^2$. By Lemma (3),

$$\int_R \varphi(x,y) P_l(x) P_m(y) dx dy = \int_R \left(\sum_{k=0}^{N-1} x^k \int_{-c}^c i^k \exp(iy\xi_2) d\nu_k(\xi_2) \right) P_l(x) P_m(y) dx dy + \quad (78)$$

$$\int_R \left(\int_{R_c} \exp(i(\xi_1 x + \xi_2 y)) x^N P_l(x) P_m(y) d\mu(\xi_1, \xi_2) \right) dx dy. \quad (79)$$

$$= \sum_{k=0}^{N-1} \left(\int_{-1}^1 x^k P_l(x) dx \right) \left(\int_{-1}^1 \int_{-c}^c i^k \exp(iy\xi_2) d\nu_k(\xi_2) \right) + \quad (80)$$

$$\int_{R_c} \left(\left(\int_{-1}^1 x^N \exp(ix\xi_1) P_l(x) dx \right) \left(\int_{-1}^1 \exp(ix\xi_1) P_m(y) dy \right) \right) d\mu(\xi_1, \xi_2). \quad (81)$$

Since, for $l \geq N$,

$$\int_{-1}^1 x^k P_l(x) dx = 0, \quad (82)$$

for all $k < l$, it follows that

$$\left| \int_R \varphi(x, y) P_l(x) P_k(y) dx dy \right| \leq |\mu|(R_c) \max_{(\xi_1, \xi_2) \in R_c} \left| \int_{-1}^1 \exp(i\xi_1 x) x^N P_l(x) dx \right| \left| \int_{-1}^1 \exp(i\xi_2 y) P_k(y) dy \right|. \quad (83)$$

A direct application of Lemma (4) yields

$$\left| \int_{-1}^1 \exp(i\xi_2 y) P_k(y) dy \right| \leq \frac{2 \left| \frac{c}{2} \right|^k}{\Gamma(k+1)} \quad (84)$$

for $|\xi_2| \leq c$. Substituting

$$x^N P_k(l) = \sum_{k=m-N}^{m+N} b_k P_k(x), \quad (85)$$

into (85), where

$$b_k = \sqrt{k + \frac{1}{2}} \int_{-1}^1 x^N P_k(x) dx, \quad (86)$$

in conjunction with Lemma (4), yields

$$\left| \int_{-1}^1 \exp(i\xi_1 x) x^N P_l(x) dx \right| \leq \sum_{k=l-N}^{l+N} \frac{2|b_k| \left| \frac{\xi_1}{2} \right|^{l+N}}{\Gamma(l+1)} \leq \frac{(4N+2) \max\{|b_k|\} \left(\frac{c}{2} \right)^{l+N}}{\Gamma(l-N+1)} \quad (87)$$

for all $|\xi_1| \leq c$. Combining this result with (84) and (83) yields (77). \square

3 Analysis of the Levin Equation

In this section, we prove the existence of a non-oscillatory solution to the two-dimensional Levin equation

$$\nabla \cdot \mathbf{p}(x, y) + i \nabla g(x, y) \cdot \mathbf{p}(x, y) = f(x, y). \quad (88)$$

on the domain R regardless of the magnitude of ∇g . Our theorems apply even in the case where g has a stationary point. Equation (88) is a scalar equation whose unknown is a vector field of two components. As a result, we are free to impose an additional relationship between the components of \mathbf{p} . For instance, we can assume that \mathbf{p} is of the form

$$\mathbf{p}(x, y) = \mathbf{v}(x, y) p(x, y) \quad (89)$$

for a given $\mathbf{v}(x, y)$ and unknown $p : \mathbb{R}^2 \rightarrow \mathbb{C}$. In this section, we prove that when \mathbf{p} takes the form

$$\mathbf{p}(x, y) = \begin{pmatrix} p(x, y) \\ 0 \end{pmatrix}, \quad (90)$$

there exists a non-oscillatory solution regardless of the magnitude of $\frac{\partial g}{\partial x}$. In fact, it is easy to see that this result holds for any choice of constant \mathbf{v} , since the theorem can be applied on a larger rectangular domain containing R , which has been rotated so that one of the sides is aligned with \mathbf{v} . This observation can be exploited numerically to accelerate the Levin method by choosing an appropriate v —see our discussion in Section (4.1).

Imposing the restriction (90) results in the equation

$$\frac{\partial p}{\partial x}(x, y) + i \frac{\partial g}{\partial x}(x, y) p(x, y) = f(x, y), \quad (91)$$

which, for each $y \in [-1, 1]$, reduces to the one dimensional Levin equation (2). We begin our analysis of (91) by considering the case where $\frac{\partial g}{\partial x}$ is constant. That is, we show the existence of a non-oscillatory solution to

$$\frac{\partial}{\partial x} p(x, y) + i\omega_1 p(x, y) = f(x, y). \quad (92)$$

This reduces the differential equation to the one which appears in [3].

For the remainder of this section, let $R = [-1, 1]^2$, and let $R_y = [-1, 1] \times \{y\}$.

Lemma 5. Suppose that $f : R \rightarrow \mathbb{C}$ admits an infinitely differentiable extension to an open neighbourhood of R , and $\omega_1 \neq 0$. Then for each $0 < \epsilon < 1$, there exists a function $p_b \in S(\mathbb{R}^2)$ such that

1. $\hat{p}_b(\xi_1, \xi_2)$ is a tempered distribution of order $(1, 0)$ supported on $[-c_f(\epsilon), c_f(\epsilon)]^2$,
2. $\left| \frac{\partial p_b}{\partial x}(x, y) + i\omega_1 p_b(x, y) \right| \leq \epsilon \|f\|_{L^\infty(R)}$ for all $(x, y) \in R$,
3. $\|p_b\|_{L^\infty(R)} \lesssim \min \left\{ 1, \frac{1}{|\omega_1|} \right\} \|f\|_{L^\infty(R)}$ and
4. $\left\| \frac{\partial}{\partial x} p_b \right\|_{L^\infty(R)} \lesssim \min \left\{ 1, \frac{1}{|\omega_1|} \right\} \|f\|_{L^\infty(R)}$.

Proof. We let $f_b \in S(\mathbb{R}^2)$ be a function with a bandlimit $W_0 = c_f(\epsilon)$ which adheres to all conditions in Definition (1) and define p_b via the formula

$$p_b(x, y) = \int_{-W_0}^{W_0} \left[\text{p.v.} \int_{-W_0}^{W_0} \frac{\hat{f}_b(\xi_1, \xi_2)}{i(\xi_1 + \omega_1)} \exp(i(\xi_1 x + \xi_2 y)) d\xi_1 \right] d\xi_2. \quad (93)$$

It is clear that p_b is a tempered distribution of order $(1, 0)$, so condition (1) above holds. Moreover, it follows that

$$\frac{\partial p_b}{\partial x}(x, y) + i\omega_1 p_b(x, y) = \int_{-W_0}^{W_0} \left[\text{p.v.} \int_{-W_0}^{W_0} \frac{i(\omega_1 + \xi_1) \hat{f}_b(\xi_1, \xi_2)}{i(\omega_1 + \xi_1)} \exp(i(\xi_1 x + \xi_2 y)) d\xi_1 \right] d\xi_2 = f_b(x, y). \quad (94)$$

Recalling from Definition (1) that

$$\|f - f_b\|_{L^\infty(R)} \leq \epsilon \|f\|_{L^\infty(R)}, \quad (95)$$

condition (2) above immediately follows. By taking the inverse Fourier transform in the variable ξ_2 in (93), we obtain the following formula

$$p_b(x, y) = \text{p.v.} \int_{-W_0}^{W_0} \frac{\hat{f}_b(\xi_1, y)}{i(\xi_1 + \omega_1)} e^{ix\xi_1} d\xi_1. \quad (96)$$

We now apply Lemma 4 from [3] to see that the bounds

$$\|p_b\|_{L^\infty(R_y)} \lesssim \min \left\{ 1, \frac{1}{|\omega_1|} \right\} \|f\|_{L^\infty(R_y)} \quad \text{and} \quad (97)$$

$$\left\| \frac{\partial}{\partial x} p_b \right\|_{L^\infty(R_y)} \lesssim \min \left\{ 1, \frac{1}{|\omega_1|} \right\} \|f\|_{L^\infty(R_y)}. \quad (98)$$

hold for each $y \in [-1, 1]$. Conclusions (3) and (4) follow by taking the supremum over $y \in [-1, 1]$ of equations (97) and (98). \square

The proceeding lemma provides a bound on the error of the approximate solution p in the case where $\frac{\partial g}{\partial x}$ is constant. We now consider (91) in the case where $\frac{\partial g}{\partial x}$ is non-constant but does not have stationary points. As with the constant coefficient case, the coefficient $\frac{\partial g}{\partial x}$ can be arbitrarily small in magnitude. We suppose that $f : R \rightarrow \mathbb{C}$ and $g : R \rightarrow \mathbb{R}$ admit infinitely differentiable extensions to open neighbourhoods of R and that the extension of $\frac{\partial g}{\partial x}$ is non-zero on this open domain containing R .

For each $y \in [-1, 1]$, we define

$$W^{(y)} = \frac{1}{2} \int_{-1}^1 \left(\frac{\partial g}{\partial x}(x, y) \right) dx. \quad (99)$$

and let

$$W_- = \min_y \{W^{(y)}\} \quad \text{and} \quad W_+ = \max_y \{W^{(y)}\}. \quad (100)$$

Moreover, we define

$$G_0 = \min_{(x,y) \in R} \left| \frac{\partial g}{\partial x}(x,y) \right|. \quad (101)$$

Further, for each $y \in [-1, 1]$, we let $u^{(y)} : R_y \rightarrow R_y$ be given by the formula

$$u^{(y)}(x) = -1 + \frac{1}{W^{(y)}} \int_{-1}^x \left(\frac{\partial g}{\partial x}(x,y) \right) dx. \quad (102)$$

Noting that since $\frac{\partial g}{\partial x}$ is non-zero in an open neighbourhood of R , it follows that, for each y in an open neighbourhood of $[-1, 1]$, $u^{(y)}$ is invertible and its inverse extends to an open neighbourhood of $[-1, 1]$. Finally, let $h : R \rightarrow R$ be defined by

$$h(z, y) = \frac{f((u^{(y)})^{-1}(z), y)}{\frac{\partial u^{(y)}}{\partial x}((u^{(y)})^{-1}(z))}. \quad (103)$$

Under the above assumptions and notations, we have the following:

Theorem 3. *For every $0 < \epsilon < 1$, there exists a function $p_b : R \rightarrow \mathbb{C}$ such that*

1. *The Fourier transform of $p_b((u^{(y)})^{-1}(z), y)$ is a tempered distribution of order $(1, 0)$ supported on $[-c_h(\epsilon), c_h(\epsilon)]^2$ where h is defined via (103),*
2. $\left| \frac{\partial p_b}{\partial x}(x, y) + i \frac{\partial g}{\partial x}(x, y) p_b(x, y) - f(x, y) \right| \lesssim \epsilon \frac{|W_+|}{G_0} \|f\|_{L^\infty(R)}$ *for all $(x, y) \in R$,*
3. $\|p_b\|_{L^\infty(R)} \lesssim \frac{|W_+|}{G_0} \min \left\{ 1, \frac{1}{|W_-|} \right\} \|f\|_{L^\infty(R)},$
4. $\left\| \frac{\partial p_b}{\partial x} \right\|_{L^\infty(R)} \lesssim \frac{|W_+|}{G_0} \min \left\{ 1, \frac{1}{|W_-|} \right\} \|f\|_{L^\infty(R)}.$

Proof. By substituting the variable $z = u^{(y)}(x)$ into (91) and noting that

$$\frac{\partial g}{\partial x}(x, y) = W^{(y)} \frac{\partial u^{(y)}}{\partial x}(x), \quad (104)$$

we obtain

$$\frac{\partial p}{\partial z}(z, y) + i\omega_1 p(z, y) = h(z, y) \quad (z, y) \in R. \quad (105)$$

Since both f and g admit infinitely differentiable extensions to open neighbourhoods of R , $u^{(y)}$ and h do as well. This means we can apply Lemma (5) to (105), which shows that there exists an entire function $p_1(z, y)$ such that

1. $\hat{p}_1(\xi_1, \xi_2)$ is a tempered distribution of order $(1, 0)$ supported on $[-c_h(\epsilon), c_h(\epsilon)]^2$,
2. $\left| \frac{\partial p_1}{\partial z}(z, y) + iW_+ p_1(z, y) \right| \lesssim \epsilon \|h\|_{L^\infty(R)}$ *for all $(z, y) \in R$,*
3. $\|p_1\|_{L^\infty(R)} \lesssim \min \left\{ 1, \frac{1}{|W_-|} \right\} \|h\|_{L^\infty(R)}$ *and*
4. $\left\| \frac{\partial p_1}{\partial x} \right\|_{L^\infty(R)} \lesssim \min \left\{ 1, \frac{1}{|W_-|} \right\} \|h\|_{L^\infty(R)}.$

Now, by defining $p_b(x, y)$ by the formula $p_b(x, y) = p_1(u^{(y)}(x), y)$, it is clear that the first conclusion of this theorem is satisfied. The other conclusions of the theorem follow from

$$\|h\|_{L^\infty(R)} = \left\| \left(\frac{\partial u^{(y)}}{\partial z} \right)^{-1} \right\|_{L^\infty(R)} \|f\|_{L^\infty(R)} \leq \frac{|W_+|}{G_0} \|f\|_{L^\infty(R)} \quad (106)$$

and the properties of p_1 listed above. \square

It is important to note that Theorem 3 does not imply that the Fourier transform of the approximate solution p_b of the two dimensional Levin equation has compact support. Instead, it only shows that

$$p_b = \langle \hat{p}_1, \eta_{(x,y)} \rangle, \quad (107)$$

where \hat{p}_1 is a tempered distribution of order $(1, 0)$ which is compactly supported and

$$\eta_{(x,y)}(\xi_1, \xi_2) = \exp(i(\xi_1 u^y(x) + \xi_2 y)). \quad (108)$$

Since p_b is the composition of the entire function p_1 and the infinitely differentiable function u^y , the magnitude of the coefficients $\{a_{ij}\}$ of the bivariate Legendre expansion decay faster than any polynomial. Moreover, (107) implies that p_b can be approximated at fixed relative precision via a Legendre expansion at a cost independent of the magnitude of $\frac{\partial g}{\partial x}$. This is clear since h is defined only in terms of f and the normalized version u^y of g , so that $c_h(\epsilon)$ is independent of the magnitude of $\frac{\partial g}{\partial x}$. As a result, the bandlimit of p_1 is independent of the magnitude of $\frac{\partial g}{\partial x}$, and by extension, so is p_b .

Our final theorem of this section applies whenever $\frac{\partial g}{\partial x}$ is of small magnitude, regardless of whether it vanishes or not.

Theorem 4. *Suppose that both $f : R \rightarrow \mathbb{C}$ and $g : R \rightarrow \mathbb{R}$ admit infinitely differentiable extensions to open neighbourhoods of R , and that*

$$G_1 = \min_{(x,y) \in R} \left| \frac{\partial g}{\partial x} \right| < \frac{1}{2}. \quad (109)$$

Let $0 < \epsilon < 1$ be given, and define an integer N given by

$$N = \left\lfloor \frac{\log(\epsilon)}{\log(2G_1)} \right\rfloor. \quad (110)$$

Then there exists a function $p_b \in C^\infty(\mathbb{R}^2)$ such that

1. The Fourier transform of p_b is a tempered distribution of order $(1, 0)$ supported on the domain

$$[-c_f(\epsilon) - N c_{\partial g/\partial x}(\epsilon), c_f(\epsilon) + N c_{\partial g/\partial x}(\epsilon)]^2, \quad (111)$$

2. $\left| \frac{\partial p_b}{\partial x}(x, y) + i \frac{\partial g}{\partial x}(x, y) b_p(x, y) - f(x, y) \right| \leq 2\epsilon \left(1 + \frac{G_1}{1-2G_1} \right) \|f\|_{L^\infty(R)}$ for all $(x, y) \in R$,
3. $\|p_b\|_{L^\infty(R)} \leq \frac{2}{1-2G_1} \|f\|_{L^\infty(R)}$ and
4. $\left\| \frac{\partial p_b}{\partial x} \right\|_{L^\infty(R)} \leq 4 \left(1 + \frac{G_1}{1-2G_1} \right) \|f\|_{L^\infty(R)}.$

Proof. We let f_b and $\frac{\partial g_b}{\partial x}$ denote the bandlimited functions of f and $\frac{\partial g}{\partial x}$ which satisfy the requirements of Definition 1. In particular, we note that $\|f_b\|_{L^\infty(R)} \leq (1 + \epsilon) \|f\|_{L^\infty(R)}$. Define the functional operator $A : L^\infty(R) \rightarrow L^\infty(R)$ via the formula

$$A[\varphi](x, y) = \int_0^x \frac{\partial g_b}{\partial x'}(x', y) \varphi(x', y) dx'. \quad (112)$$

Moreover, let

$$h(x, y) = \int_0^x f(x', y) dx' \quad (113)$$

and

$$p_b(x, y) = \sum_{k=0}^N A^k [h](x, y), \quad (114)$$

where A^0 is the identity and A^k denotes repeated application of the operator A . Clearly,

$$\|A\|_\infty \leq \left\| \frac{\partial g_b}{\partial x} \right\|_{L^\infty(R)} \leq G_2 < 1, \quad (115)$$

so

$$\|p_b\|_{L^\infty(R)} \leq \left(\sum_{k=0}^N \|A\|_\infty^k \right) \|h\|_{L^\infty(R)} \quad (116)$$

$$\leq \frac{1+G_2^{N+1}}{1-G_2} \|f\|_{L^\infty(R)} \quad (117)$$

$$\leq \frac{1+\epsilon}{1-2G_1} \|f\|_{L^\infty(R)}. \quad (118)$$

Conclusion (2) of the theorem follows. Now it follows from (114) that

$$\frac{\partial}{\partial x} A^0[h](x, y) = \frac{\partial h}{\partial x}(x, y) = f_b(x, y), \quad (119)$$

$$\frac{\partial}{\partial x} A^k[h](x) = -i \frac{\partial g_b}{\partial x} A^{k-1}[h](x, y) \quad \text{for } k \geq 1. \quad (120)$$

Therefore,

$$\frac{\partial p_b}{\partial x}(x, y) = f_b(x, y) - i \frac{\partial g_b}{\partial x}(x, y) \sum_{k=0}^{N-1} A^k[h](x, y) \quad (121)$$

$$= f_b(x, y) - i \frac{\partial g_b}{\partial x}(x, y) \sum_{k=0}^N A^k[h](x, y) + i \frac{\partial g_b}{\partial x}(x, y) A^N[h](x, y) \quad (122)$$

$$= f_b(x, y) - i \frac{\partial g}{\partial x}(x, y) p_b(x, y) + i \frac{\partial g_b}{\partial x}(x, y) A^N[h](x, y) \quad (123)$$

for all $(x, y) \in R$. Further, (123) implies

$$\left\| \frac{\partial p_b}{\partial x} \right\|_{L^\infty(R)} \leq \|f_b\|_{L^\infty(R)} + \left\| \frac{\partial g_b}{\partial x} \right\|_{L^\infty(R)} \|p_b\|_{L^\infty(R)} + 2\epsilon \|f_b\|_{L^\infty(R)} \quad (124)$$

$$\leq \left((1+\epsilon) + G_1 \frac{2}{1-2G_1} + 2\epsilon \right) \|f\|_{L^\infty(R)} \quad (125)$$

$$\leq \left(4 + \frac{2G_1}{1-2G_1} \right) \|f\|_{L^\infty(R)}, \quad (126)$$

which shows conclusion (3) in the statement of the theorem. Again utilizing (123),

$$\left| \frac{\partial p_b}{\partial x}(x, y) + i \frac{\partial g_b}{\partial x}(x, y) p_b(x, y) - f(x, y) \right| \leq \left| \frac{\partial p_b}{\partial x}(x, y) + i \frac{\partial g_b}{\partial x}(x, y) p_b(x, y) - f_b(x, y) \right| + |f_b(x, y) - f(x, y)| \quad (127)$$

$$\leq \left| i \frac{\partial g_b}{\partial x}(x, y) A^N[h](x, y) \right| + \epsilon \|f\|_{L^\infty(R)} \quad (128)$$

$$\leq (1+\epsilon)^{N+1} G_1^{N+1} \|f_b\|_{L^\infty(R)} + \epsilon \|f\|_{L^\infty(R)} \quad (129)$$

$$\leq 2\epsilon \|f_b\|_{L^\infty(R)}. \quad (130)$$

Applying both (118) and (126), we obtain

$$\left| \frac{\partial p_b}{\partial x}(x, y) + i \frac{\partial g}{\partial x}(x, y) p_b(x, y) - f(x, y) \right| \leq \left| \frac{\partial p_b}{\partial x}(x, y) + i \frac{\partial g_b}{\partial x}(x, y) p_b(x, y) - f(x, y) \right| + \quad (131)$$

$$\left| i \frac{\partial g_b}{\partial x}(x, y) p_b(x, y) - i \frac{\partial g}{\partial x}(x, y) p_b(x, y) \right| \quad (132)$$

$$\leq 2\epsilon \|f\|_{L^\infty(R)} + \epsilon \|p_b\|_{L^\infty(R)} \left\| \frac{\partial g}{\partial x} \right\|_{L^\infty(R)} \quad (133)$$

$$\leq \left(2 + \frac{2G_1}{1-2G_1} \right) \epsilon \|f\|_{L^\infty(R)}, \quad (134)$$

which establishes the second conclusion. It remains to prove the first conclusion. We first observe that the Fourier transform of the function h , as defined in (113), is given by

$$\hat{h}(\xi_1, \xi_2) = \frac{1}{4\pi^2} \int_{-\infty}^{\infty} \int_{-\infty}^{\infty} \left[\int_0^x f_b(x', y) dx' \right] \exp(i(x\xi_1 + y\xi_2)) dx dy \quad (135)$$

$$= \text{p.v.} \frac{\hat{f}_b(\xi_1, \xi_2)}{i\xi_1} + \frac{\delta(\xi_1)}{2\pi} \left(\int_0^{\infty} \hat{f}_b(x, \xi_2) dx + \int_{-\infty}^0 \hat{f}_b(x, \xi_2) dx \right) \quad (136)$$

where $\delta(\xi_1)$ is the Dirac-Delta distribution. Clearly, (136) is a tempered distribution of order $(1, 0)$ supported on the domain $[-c_f(\epsilon), c_f(\epsilon)]^2$. Note that if the Fourier transform of a function $\varphi \in C^\infty(\mathbb{R}^2)$ is a tempered distribution of order $(1, 0)$ supported on the domain $[-c, c]^2$, then it's convolution with the function $\frac{\partial g_b}{\partial x} \in S(\mathbb{R}^2)$ is a tempered distribution of order $(0, 0)$ supported on the domain $[-c - c_{\partial g/\partial x}(\epsilon), c + c_{\partial g/\partial x}(\epsilon)]^2$. Note that $A[\varphi]$ is the integral over x of the aforementioned convolution, and hence its Fourier transform is a tempered distribution of order $(1, 0)$ supported on the same domain. It follows inductively that, for all k , the Fourier transform of $A^k[h]$ is a tempered distribution of order $(1, 0)$ with support on the domain

$$[-c_f(\epsilon) - kc_{\partial g/\partial x}(\epsilon), c_f(\epsilon) + kc_{\partial g/\partial x}(\epsilon)]^2. \quad (137)$$

Combining the above with (114) yields the first conclusion, and completes our proof. \square

4 Numerical Aspects of the Levin Method

In this section, we give an argument which shows that when the Levin equation (91) is discretized using a bivariate Chebyshev spectral collocation method and the resulting linear system is solved via a truncated singular value decomposition, a high-accuracy solution is obtained, regardless of the magnitude of $\frac{\partial g}{\partial x}$ or whether or not it has stationary points. Here, we represent the solution p using a bivariate Chebyshev expansion of order n which utilizes $M = \frac{(n+1)(n+2)}{2}$ basis functions. However, we require that the Levin equation holds on the nodes of a Chebyshev tensor product quadrature of order

$$k = \lceil \sqrt{2M} \rceil. \quad (138)$$

We take this approach since the Levin equation involves the product of $\frac{\partial g}{\partial x}$ and p , which is represented by a bivariate Chebyshev expansion of order $2M$. While the rigorous bounds presented here depend on the value of k given by (138), in practice there is negligible impact of imposing conditions on only l collocation nodes, where l slightly exceeds M .

We begin by providing an analysis on the error of the computed integral value under the assumption that $\frac{\partial g}{\partial x}$ is strictly non-zero. Following this, we treat the case in which $\frac{\partial g}{\partial x}$ is of small magnitude on the solution domain, possibly with zeroes. Finally, we close this section by discussing how a particular choice of \mathbf{v} from (90) can be used to numerically accelerate the Levin method.

Throughout this section, we suppose that $f : R \rightarrow \mathbb{C}$ and $g : R \rightarrow \mathbb{R}$ admit infinitely differentiable extensions to open neighbourhoods of R , and that $0 < \epsilon < 1$. Moreover, we define

$$G_0 = \min_{(x,y) \in R} \left| \frac{\partial g}{\partial x}(x, y) \right| \quad \text{and} \quad G_1 = \max_{(x,y) \in R} \left| \frac{\partial g}{\partial x}(x, y) \right|, \quad (139)$$

as well as

$$W_- = \frac{1}{2} \min_{y \in [-1, 1]} \int_{-1}^1 \left(\frac{\partial g}{\partial x}(x, y) \right) dx \quad \text{and} \quad W_+ = \frac{1}{2} \max_{y \in [-1, 1]} \int_{-1}^1 \left(\frac{\partial g}{\partial x}(x, y) \right) dx. \quad (140)$$

We first suppose that $G_0 > 0$; among other things, this assumption ensures that there are no zeroes of $\frac{\partial g}{\partial x}$ in R . By Theorem 3, there exists a bandlimited function $p_b : R \rightarrow \mathbb{C}$ such that

$$\left| \frac{\partial p_b}{\partial x}(x, y) + i \frac{\partial g}{\partial x}(x, y) p_b(x, y) - f(x, y) \right| \lesssim \epsilon \frac{|W_+|}{G_0} \|f\|_{L^\infty(R)} \text{ for all } (x, y) \in R, \quad (141)$$

$$\|p_b\|_{L^\infty(R)} \lesssim \frac{|W_+|}{G_0} \min \left\{ 1, \frac{1}{|W_-|} \right\} \|f\|_{L^\infty(R)}, \quad (142)$$

$$\left\| \frac{\partial p_b}{\partial x} \right\|_{L^\infty(R)} \lesssim \frac{|W_+|}{G_0} \min \left\{ 1, \frac{1}{|W_-|} \right\} \|f\|_{L^\infty(R)}. \quad (143)$$

It follows from the discussion in Section 2.2 that we can choose an integer n independent of $|W_+|, |W_-|$ and G_1 such that

$$\|P_n[f] - f\|_{L^\infty(R)} \leq \epsilon \|f\|_{L^\infty(R)}, \quad (144)$$

$$\left\| P_n \left[\frac{\partial g}{\partial x} \right] - \frac{\partial g}{\partial x} \right\|_{L^\infty(R)} \leq \epsilon \left\| \frac{\partial g}{\partial x} \right\|_{L^\infty(R)}, \quad (145)$$

$$\|P_n[p_b] - p_b\|_{L^\infty(R)} \leq \epsilon \|p_b\|_{L^\infty(R)}. \quad (146)$$

If $0 < \epsilon < 1$, then

$$\left\| P_n \left[\frac{\partial g}{\partial x} \right] \right\|_{L^\infty(R)} \leq 2 \left\| \frac{\partial g}{\partial x} \right\|_{L^\infty(R)}, \quad (147)$$

$$\|P_n[p_b]\|_{L^\infty(R)} \leq 2 \|p_b\|_{L^\infty(R)}. \quad (148)$$

The above inequalities together with (33) show that we can choose integer n so that

$$\left\| \frac{\partial}{\partial x} P_n[p_b] + iP_n \left[\frac{\partial g}{\partial x} \right] P_n[p_b] - \left(\frac{\partial p_b}{\partial x} + i \frac{\partial g}{\partial x} p_b \right) \right\|_{L^\infty(R)} \leq \epsilon \left\| \frac{\partial p_b}{\partial x} \right\|_{L^\infty(R)} + 4\epsilon G_1 \|p_b\|_{L^\infty(R)} \quad (149)$$

$$\lesssim \epsilon (1 + 4G_1) \frac{|W_+|}{G_0} \min \left\{ 1, \frac{1}{|W_-|} \right\} \|f\|_{L^\infty(R)}. \quad (150)$$

Combining (141) and (150), we obtain

$$\left| \frac{\partial}{\partial x} P_n[p_b](x, y) + P_n \left[\frac{\partial g}{\partial x} \right] (x, y) P_n[p_b](x, y) - f(x, y) \right| \lesssim \epsilon \left(1 + (1 + G_1) \min \left\{ 1, \frac{1}{|W_-|} \right\} \right) \frac{|W_+|}{G_0} \|f\|_{L^\infty(R)} \quad (151)$$

for all $(x, y) \in R$.

We define the $k^2 \times k^2$ matrix \mathcal{G} via

$$\mathcal{G} = \text{diag} \left[\frac{\partial g}{\partial x} \right] \quad (152)$$

where k is given by (138). It follows from (151) that

$$(\mathcal{D}_x^k + i\mathcal{G})[p_b] = [f] + [\delta], \quad (153)$$

where

$$\|[p_b]\| \lesssim \frac{|W_+|}{G_0} \min \left\{ 1, \frac{1}{|W_-|} \right\} \|f\|_{L^\infty(R)} \quad (154)$$

and

$$\|[\delta]\| \lesssim \epsilon \left(1 + (1 + G_1) \min \left\{ 1, \frac{1}{|W_-|} \right\} \right) \frac{|W_+|}{G_0} \|f\|_{L^\infty(R)}. \quad (155)$$

The bounds on $\|[p_b]\|$ and $\|[\delta]\|$ are consequence of (142) and (151), respectively. It follows from (154) and (155), as well as the obvious inequality

$$\|\mathcal{D}_x^k + i\mathcal{G}\| \leq \max \{G_1, k^2\}, \quad (156)$$

that

$$\|[\delta]\| \lesssim \epsilon \max \{G_1, k^2\} \|[p_b]\|. \quad (157)$$

By Lemma 1, solving the linear system

$$(\mathcal{D}_x^k + i\mathcal{G})[p_1] = [f] \quad (158)$$

via a singular value decomposition truncated at precision on the order of $\epsilon \|\mathcal{D}_x^k + i\mathcal{G}\|$ yields a solution $[p_1]$ such that

$$[p_1] \lesssim [p_b] \lesssim \frac{|W_+|}{G_0} \min \left\{ 1, \frac{1}{|W_-|} \right\} \|f\|_{L^\infty(R)} \quad (159)$$

and therefore

$$\|(\mathcal{D}_x^k + i\mathcal{G})[p_1] - [f]\| \lesssim \|\mathcal{D}_x^k + i\mathcal{G}\| \|p_1\| \quad (160)$$

$$\lesssim \epsilon \frac{|W_+|}{G_0} \max\{G_1, k^2\} \min \left\{ 1, \frac{1}{|W_-|} \right\} \|f\|_{L^\infty(R)}. \quad (161)$$

Since the Chebyshev polynomials are bounded in $L^\infty(R)$ with norm 1, it follows from (159) that

$$\|p_1\|_{L^\infty(R)} \lesssim \frac{|W_+|}{G_0} \min \left\{ 1, \frac{1}{|W_-|} \right\} \|f\|_{L^\infty(R)}, \quad (162)$$

and from (161) that

$$\|\delta_1\|_{L^\infty(R)} \lesssim \epsilon \frac{|W_+|}{G_0} \max\{G_1, k^2\} \min \left\{ 1, \frac{1}{|W_-|} \right\} \|f\|_{L^\infty(R)}, \quad (163)$$

where p_1 and δ_1 are n^{th} order bivariate Chebyshev expansions which agree with the values of $[p_1]$ and $(\mathcal{D}_x^k + i\mathcal{G})[p_1] - [f]$ respectively at the collocation nodes. Moreover, we clearly have

$$\left[\frac{\partial p_1}{\partial x} + i \frac{\partial g}{\partial x} p_1 \right] = [f + \delta_1] \quad (164)$$

and

$$P_n \left[\frac{\partial p_1}{\partial x} + i \frac{\partial g}{\partial x} p_1 \right] (x, y) = P_n[f + \delta_1](x, y). \quad (165)$$

Since p_1 and δ_1 are n^{th} bivariate Chebyshev expansions of the form (27), it follows that $P_n[p_1] = p_1$ and similarly for δ_1 . A simple application of (30) and (32) yields

$$\left\| P_n \left[\frac{\partial p_1}{\partial x} + i \frac{\partial g}{\partial x} p_1 \right] - \left(\frac{\partial p_1}{\partial x} + i \frac{\partial g}{\partial x} p_1 \right) \right\|_{L^\infty(R)} \lesssim \epsilon G_1 \|p_1\|_{L^\infty(R)} \quad (166)$$

and

$$\|P_n[f + \delta_1] - (f + \delta_1)\|_{L^\infty(R)} \lesssim \epsilon \|f\|_{L^\infty(R)}. \quad (167)$$

Finally, it follows from (163), (165), (166) and (167), that

$$\left| \frac{\partial p_1}{\partial x}(x, y) + i \frac{\partial g}{\partial x}(x, y) p_1(x, y) - f(x, y) \right| \lesssim \epsilon A_1 \|f\|_{L^\infty(R)}, \quad (168)$$

where

$$A_1 = \left(1 + \frac{G_1}{G_0} + \frac{1}{G_0} \max\{G_1, k^2\} \right) |W_+| \min \left\{ 1, \frac{1}{|W_-|} \right\}. \quad (169)$$

Utilizing this, we will now analyze the error in the value of the integral computed via the Levin method. Let

$$I = \int_{-1}^1 \int_{-1}^1 f(x, y) \exp(ig(x, y)) dx dy \quad (170)$$

be the true value for the oscillatory integral, and consider the estimate I_1 given by

$$I_1 = \int_{-1}^1 \int_{-1}^1 \frac{\partial}{\partial x} (p_1(x, y) \exp(ig(x, y))) dx dy. \quad (171)$$

We have

$$|I_1 - I| = \left| \int_{-1}^1 \int_{-1}^1 \left(\frac{\partial p_1}{\partial x}(x, y) + i \frac{\partial g}{\partial x}(x, y) p_1(x, y) - f(x, y) \right) \exp(ig(x, y)) dx dy \right|, \quad (172)$$

$$\lesssim \epsilon A_1 \|f\|_{L^\infty(R)} \quad (173)$$

which holds in the case in which $G_0 > 0$. Note that $|W_+| \min \left\{ 1, \frac{1}{|W_-|} \right\}$ is bounded independent by the magnitude of $\frac{\partial g}{\partial x}$, provided that $\frac{\partial g}{\partial x}$ does not vary rapidly in y . Moreover, G_1/G_0 remains small provided that $\frac{\partial g}{\partial x}$ does not vary rapidly in x or y . These assumptions are, of course, reasonable when analyzing an adaptive scheme. Therefore, (173) implies that when $\frac{\partial g}{\partial x}$ varies slowly over the domain of interest, the error on the integral estimate computed via the Levin method is bounded independent of the magnitude of $\frac{\partial g}{\partial x}$.

We now consider the case in which G_1 is small; in particular, we suppose that $G_1 < \frac{1}{4}$. Deploying Theorem 4, we obtain the existence of a bandlimited function p_b with bandlimit

$$[-c_f(\epsilon) - N c_{\partial g/\partial x}(\epsilon), c_f(\epsilon) + N c_{\partial g/\partial x}(\epsilon)]^2, \quad (174)$$

where

$$N = \left\lfloor \frac{\log(\epsilon)}{\log(2G_1)} \right\rfloor \quad (175)$$

such that

$$\left| \frac{\partial p_b}{\partial x}(x, y) + i \frac{\partial g}{\partial x}(x, y) p_b(x, y) \right| \leq 2\epsilon \left(\frac{2}{1 - 2G_1} \right) \|f\|_{L^\infty(R)} \quad (176)$$

and

$$\left\| \frac{\partial p_b}{\partial x} \right\|_{L^\infty(R)} \leq 4 \left(1 + \frac{G_1}{1 - 2G_1} \right) \|f\|_{L^\infty(R)}. \quad (177)$$

Since $G_1 < \frac{1}{4}$, it follows that (174) is bounded and so the coefficient $\{a_{ij}\}$ of the bivariate Chebyshev expansion are bounded by a rapidly decaying function which is independent of G_1 . Proceeding just as above, we can choose n independent of G_1 such that

$$\left\| \frac{\partial}{\partial x} P_n[p_b] + iP_n \left[\frac{\partial g}{\partial x} \right] P_n[p_b] - \left(\frac{\partial p_b}{\partial x} + i \frac{\partial g}{\partial x} p_b \right) \right\|_{L^\infty(R)} \lesssim \epsilon \left(1 + \frac{2G_1}{1 - 2G_1} \right) \|f\|_{L^\infty(R)} \quad (178)$$

Defining $[p_b]$, $[\delta]$ and \mathcal{G} as before, we see that

$$\|[\delta]\| \lesssim \epsilon \left(\frac{4G_1}{1 - 2G_1} \right) \|f\|_{L^\infty(R)} \quad (179)$$

and

$$\|(\mathcal{D}_x^k + \mathcal{G})[p_b]\| \lesssim \max\{G_1, k^2\} \frac{2}{1 - 2G_1} \|f\|_{L^\infty(R)}. \quad (180)$$

Solving the system

$$(\mathcal{D}_x^k + i\mathcal{G})[p_1] = [f] \quad (181)$$

via a singular value decomposition truncated at precision on the order of $\epsilon \|\mathcal{D}_x^k + i\mathcal{G}\|$ yields a solution $[p_1]$ such that

$$\|[p_1]\| \lesssim \frac{2}{1 - 2G_1} \|f\|_{L^\infty(R)} \quad (182)$$

and

$$\|(\mathcal{D}_x^k + \mathcal{G})[p_b] - [f]\| \lesssim \epsilon \max\{G_1, k^2\} \frac{2}{1 - 2G_1} \|f\|_{L^\infty(R)}. \quad (183)$$

Defining p_1 and δ as before, we then obtain the bound

$$\left| \frac{\partial p_1}{\partial x}(x, y) + i \frac{\partial g}{\partial x}(x, y) p_1(x, y) - f(x, y) \right| \lesssim \epsilon A_2 \|f\|_{L^\infty(R)}, \quad (184)$$

where

$$A_2 = \max\{G_1, k^2\} \frac{2}{1 - 2G_1} + \frac{1}{1 - 2G_1} \quad (185)$$

which holds for all $(x, y) \in [-1, 1]$. Applying the same procedure as above, we can conclude that

$$|I_1 - I| \lesssim \epsilon A_2 \|f\|_{L^\infty([-1,1]^2)}. \quad (186)$$

Since we are considering the case where G_1 is small, it follows that the constant term A_2 is small as well. This result holds when $\frac{\partial g}{\partial x}$ is uniformly small over the domain of interest,

independent on how rapidly it may vary.

4.1 Numerical acceleration via a rotated domain

To mitigate the effect of low frequency breakdown, it is advantageous to maximize the $\nabla g \cdot \mathbf{p}$ term in (88). In Section (3), we deduced that the Levin equation admits well-behaved solutions regardless of the magnitude of ∇g , even in the presence of stationary points. This scheme only works adaptively since we can continually subdivide the domain until we are solving the equation on a region in which ∇g is approximately constant.

Throughout Section (3), we opted to solve the two dimensional Levin equation under a certain restriction of the vector-field solution \mathbf{p} , namely (90). We noted that we could more generally restrict ourselves to solutions of the form

$$\mathbf{p}(x, y) = \mathbf{v}(x, y)p(x, y) \quad (187)$$

for any sufficiently well-behaved vector field $\mathbf{v}(x, y)$. In order to maximize $\nabla g \cdot \mathbf{p}$, it is natural to choose $\mathbf{v}(x, y) = \nabla g(x, y)$. This results in the reduced Levin equation

$$(\nabla g(x, y) \cdot \mathbf{D} + (\Delta g + i\|\nabla g(x, y)\|^2)) p(x, y) = f(x, y) \quad (188)$$

where $\mathbf{D} = \begin{pmatrix} \frac{\partial}{\partial x} & \frac{\partial}{\partial y} \end{pmatrix}$. Since ∇g is approximately constant, $\Delta g \approx 0$. This reduces the equation to the same form as (91) while also maximizing the $\nabla g \cdot \mathbf{p}$ term of (88). Introducing a change of coordinates

$$\begin{pmatrix} x' \\ y' \end{pmatrix} = \begin{pmatrix} \frac{\partial g}{\partial x} & \frac{\partial g}{\partial y} \\ -\frac{\partial g}{\partial y} & \frac{\partial g}{\partial x} \end{pmatrix} \begin{pmatrix} x \\ y \end{pmatrix}, \quad (189)$$

it follows that

$$\nabla_{(x', y')} g(x', y') = \begin{pmatrix} 1 \\ 0 \end{pmatrix} \quad (190)$$

for all (x', y') . Then (188) becomes

$$\frac{\partial}{\partial x'} p(x', y') + ip(x', y') = f(x', y'), \quad (191)$$

analogous to (92) in the case where $\omega_1 = 1$. Applying Lemma 5 yields a solution p subject to relatively tight and clean bounds. Moreover, since $G_1 > 0$, the coefficient A_1 , given by (169), is minimized, resulting in minimal error in the integral estimate (173).

5 Algorithm Description

In this section, we describe a resonance-free two-dimensional adaptive Levin method for the numerical evaluation of integrals of the form (5). We begin in Section (5.1) by reviewing the algorithm used to compute the one-dimensional integral (1) introduced in [3], which is a component of the scheme of this paper. We then describe the algorithm of this paper that approximates (5) in Section (5.2). Finally, we close with Section 5.3 which gives a brief review of the adaptive Gauss-Legendre algorithm used to numerically compute reference values in the experiments of this paper.

5.1 The Adaptive Levin Method in 1D

In this subsection, we describe the adaptive Levin method in one-dimension, introduced in [3], for the numerical calculation of integrals of the form

$$\int_a^b f(x) e^{ig(x)} dx. \quad (192)$$

The algorithm operates by adaptively applying a base routine which computes an estimate of

$$\int_{a_0}^{b_0} f(x) e^{ig(x)} dx \quad (193)$$

for some subinterval $[a_0, b_0] \subset [a, b]$. The adaptive base routine takes as input the interval $[a_0, b_0]$, an integer k (controlling the number of Chebyshev nodes used to discretize the one-dimensional Levin equation), the k extremal Chebyshev nodes $\{t_{i,k}^{\text{cheb}}\}_{i=1}^k$ on the interval $[a_0, b_0]$, and the vectors of values $[f]$ and $[g]$ providing the values of the functions f and g on the Chebyshev nodes.

The base algorithm proceeds as follows:

1. Estimate the vector of values $[g']$ by applying the one-dimensional spectral differentiation matrix \mathcal{D}_k to the vector of values $[g]$. That is,

$$\begin{pmatrix} g'(t_{1,k}^{\text{cheb}}) \\ \vdots \\ g'(t_{k,k}^{\text{cheb}}) \end{pmatrix} = \mathcal{D}_k \begin{pmatrix} g(t_{1,k}^{\text{cheb}}) \\ \vdots \\ g(t_{k,k}^{\text{cheb}}) \end{pmatrix}. \quad (194)$$

2. Form the $k \times k$ matrix

$$\mathcal{A} = \mathcal{D}_k + i \begin{pmatrix} g'(t_{1,k}^{\text{cheb}}) & & & \\ & \ddots & & \\ & & g'(t_{k,k}^{\text{cheb}}) & \end{pmatrix} \quad (195)$$

so that $\mathcal{A}[p] = [f]$, which discretizes (2).

3. Construct a singular value decomposition

$$\mathcal{A} = \begin{pmatrix} | & & | \\ \mathbf{u}_1 & \cdots & \mathbf{u}_k \\ | & & | \end{pmatrix} \begin{pmatrix} \sigma_1 & & & \\ & \sigma_2 & & \\ & & \ddots & \\ & & & \sigma_k \end{pmatrix} \begin{pmatrix} | & & | \\ \mathbf{v}_1 & \cdots & \mathbf{v}_k \\ | & & | \end{pmatrix}^T \quad (196)$$

of the matrix \mathcal{A} .

4. Find the least integer $1 \leq l \leq k$ such that $\sigma_l \leq \epsilon_0 \|\mathcal{A}\|$, where ϵ_0 is machine zero. If no such integer exists, then return the estimate 0 for (193).
5. Approximate the vector of values $[p]$ of the solution p to (2) via

$$[p] = \begin{pmatrix} | & & | \\ \mathbf{v}_1 & \cdots & \mathbf{v}_l \\ | & & | \end{pmatrix} \begin{pmatrix} \frac{1}{\sigma_1} & & & \\ & \frac{1}{\sigma_2} & & \\ & & \ddots & \\ & & & \frac{1}{\sigma_l} \end{pmatrix} \begin{pmatrix} | & & | \\ \mathbf{u}_1 & \cdots & \mathbf{u}_l \\ | & & | \end{pmatrix}^T [f]. \quad (197)$$

Then the entries of the vector $[p]$ of (197) approximate the values of a function p such that

$$\frac{d}{dx} (p(x) \exp(ig(x))) = f(x) \exp(ig(x)) \quad (198)$$

at the Chebyshev extremal nodes on the interval $[a_0, b_0]$.

6. Return the estimate

$$p(t_{k,k}^{\text{cheb}}) \exp(ig(t_{k,k}^{\text{cheb}})) - p(t_{1,k}^{\text{cheb}}) \exp(ig(t_{1,k}^{\text{cheb}})) \quad (199)$$

for the approximate value of (193).

The adaptive algorithm takes as input the interval $[a, b]$, a tolerance parameter $\epsilon > 0$, an integer k (controlling the number of Chebyshev nodes used to discretize the one-dimensional Levin equation), and the vectors $[f]$ and $[g]$ of values of f and g at the Chebyshev nodes on $[a, b]$.

The algorithm maintains an estimate I for (192), as well as a stack of subintervals. Initially, this interval stack contains only the entire interval $[a, b]$ and the initial estimate I is set to 0. The following steps are repeated as long as the stack is non-empty:

1. Remove a subrectangle $[a_0, b_0]$ from the stack of subintervals.

2. Compute an estimate

$$I_0 = \int_{a_0}^{b_0} f(x) \exp(ig(x)) dx \quad (200)$$

over the entire subrectangle using the base routine described above.

3. Calculate estimates

$$I_1 = \int_{a_0}^{c_0} f(x) \exp(ig(x)) dx \quad \text{and} \quad I_2 = \int_{c_0}^{b_0} f(x) \exp(ig(x)) dx \quad (201)$$

where $c_0 = \frac{a_0+b_0}{2}$ using the base routine described above.

4. If $|I_0 - (I_1 + I_2)| < \epsilon$, then update the current estimate $I \leftarrow I + I_0$. Otherwise, add $[a_0, c_0]$ and $[c_0, b_0]$ to the stack of rectangles.

In the end, the algorithm returns an estimate I for (5).

5.2 The Adaptive Levin Method in 2D

In this section, we provide a description of the algorithm of this paper – a resonance-free adaptive Levin method in two dimensions for the numerical calculation of integrals of the form

$$\int_R f(x, y) \exp(ig(x, y)) dx dy. \quad (202)$$

Note that the algorithm can be trivially modified to handle integrals of the form

$$\int_R f(x, y) \sin(g(x, y)) dx dy \quad \text{or} \quad \int_R f(x, y) \cos(g(x, y)) dx dy. \quad (203)$$

The algorithm operates by adaptively applying a base routine which computes an estimate of

$$\int_{R_0} f(x, y) e^{ig(x, y)} dx dy \quad (204)$$

over some subrectangle $R_0 \subset R$. The base routine operates by solving either

$$\frac{\partial p}{\partial x}(x, y) + i \frac{\partial g}{\partial x}(x, y)p(x, y) = f(x, y) \quad (205)$$

or

$$\frac{\partial p}{\partial y}(x, y) + i \frac{\partial g}{\partial y}(x, y)p(x, y) = f(x, y). \quad (206)$$

In solving one of these equations, the boundary integral (9) reduces to

$$\int_{R_0} f(x, y) e^{ig(x, y)} dx dy = \int_c^d p(b, y) \exp(ig(b, y)) dy - \int_c^d p(a, y) \exp(ig(a, y)) dy \quad (207)$$

or

$$\int_{R_0} f(x, y) e^{ig(x, y)} dx dy = \int_a^b p(x, d) \exp(ig(x, d)) dx - \int_a^b p(x, c) \exp(ig(x, c)) dx \quad (208)$$

respectively. We define the constants

$$M_1 = \min \text{abs} \left[\frac{\partial g}{\partial x} \right] \quad \text{and} \quad M_2 = \min \text{abs} \left[\frac{\partial g}{\partial y} \right] \quad (209)$$

and solve (205) in the case where $M_1 > M_2$ and we solve (206) otherwise. Here we describe the base algorithm in the first case, and the description the second case is entirely analogous. In this case, the boundary integral (9) reduces to

The base routine takes as input the subrectangle R_0 , an integer k_{cheb} controlling the number of Chebyshev nodes used to construct the tensor product quadrature, an integer n_{base} specifying the maximum order of the polynomials used to represent the solution p , an integer m_{levin} specifying the number of interpolation points along each section of ∂R_0 , as well as the vectors of values $[f]$, $[g]$, $\left[\frac{\partial g}{\partial x} \right]$ and $\left[\frac{\partial g}{\partial y} \right]$. The base routine proceeds as follows;

1. Construct the $k^2 \times k^2$ matrix

$$\mathcal{A} = \mathcal{D}_x^k + i \left(\text{diag} \left[\frac{\partial g}{\partial x} \right] \right) \quad (210)$$

which discretizes (1).

2. Construct a singular value decomposition

$$\mathcal{A} = \begin{pmatrix} & & \\ \mathbf{u}_1 & \cdots & \mathbf{u}_{k^2} \\ & & \end{pmatrix} \begin{pmatrix} \sigma_1 & & & \\ & \sigma_2 & & \\ & & \ddots & \\ & & & \sigma_{k^2} \end{pmatrix} \begin{pmatrix} & & \\ \mathbf{v}_1 & \cdots & \mathbf{v}_{k^2} \\ & & \end{pmatrix}^T \quad (211)$$

of the matrix \mathcal{A} .

3. Find the least integer $1 \leq l \leq k^2$ such that $\sigma_l \geq \|\mathcal{A}\|_F \epsilon_0$ where ϵ_0 is machine zero. If no such integer exists, return the estimate 0 for (204).
4. Approximate the vector values $[p]$ of the solution p to (??) via

$$[p] = \begin{pmatrix} & & \\ \mathbf{v}_1 & \cdots & \mathbf{v}_l \\ & & \end{pmatrix} \begin{pmatrix} \frac{1}{\sigma_1} & & & \\ & \frac{1}{\sigma_2} & & \\ & & \ddots & \\ & & & \frac{1}{\sigma_l} \end{pmatrix} \begin{pmatrix} & & \\ \mathbf{u}_1 & \cdots & \mathbf{u}_l \\ & & \end{pmatrix}^T [f]. \quad (212)$$

5. Using the vector of values $[p]$, interpolate to an m -point grid of Chebyshev nodes on the relevant sections of ∂R_0 , and similarly for $[g]$. That is, obtain the vectors

$$\begin{pmatrix} p(a_0, y_{1,m}^{\text{cheb}}) \\ p(a_0, y_{2,m}^{\text{cheb}}) \\ \vdots \\ p(a_0, y_{m,m}^{\text{cheb}}) \end{pmatrix}, \quad \begin{pmatrix} p(b_0, y_{1,m}^{\text{cheb}}) \\ p(b_0, y_{2,m}^{\text{cheb}}) \\ \vdots \\ p(b_0, y_{m,m}^{\text{cheb}}) \end{pmatrix}, \quad \begin{pmatrix} g(a_0, y_{1,m}^{\text{cheb}}) \\ g(a_0, y_{2,m}^{\text{cheb}}) \\ \vdots \\ g(a_0, y_{m,m}^{\text{cheb}}) \end{pmatrix} \quad \text{and} \quad \begin{pmatrix} g(b_0, y_{1,m}^{\text{cheb}}) \\ g(b_0, y_{2,m}^{\text{cheb}}) \\ \vdots \\ g(b_0, y_{m,m}^{\text{cheb}}) \end{pmatrix}, \quad (213)$$

where $\{y_{i,m}^{\text{cheb}}\}_{i=1}^m$ is the m -point grid of Chebyshev nodes over the interval $[a_0, b_0]$.

6. Use the provided external subroutine to evaluate the function g on the two m -point grids of Chebyshev nodes $\{(a_0, y_{i,m}^{\text{cheb}})\}_{i=1}^m$, and $\{(b_0, y_{i,m}^{\text{cheb}}, c_0)\}_{i=1}^m$.

7. Return the estimate (9) by applying the one-dimensional adaptive Levin algorithm as described in Section (5.1) to the one-dimensional integrals of (207)

The algorithm proper takes a tolerance parameter $\epsilon > 0$, the domain endpoints $a < b$ and $c < d$, an integer k specifying the number of discretization nodes, an integer n specifying the order of the polynomial expansion representation, and an external subroutine which returns the values of the functions f , g and (optionally) $\frac{\partial g}{\partial x}$ and $\frac{\partial g}{\partial y}$.

The algorithm maintains an estimate I for (5), as well as a stack of subrectangles. Initially, the stack only contains the full rectangle R and the initial estimate I is set to 0. The following steps are repeated as long as the stack is non-empty:

1. Remove a subrectangle $R_0 = [a_0, b_0] \times [c_0, d_0]$ from the stack of domains.
2. Use the external subroutine supplied to evaluate the functions f , g , $\frac{\partial g}{\partial x}$ and $\frac{\partial g}{\partial y}$ at the Chebyshev tensor product quadrature $\{(x_i^{\text{cheb}}, y_j^{\text{cheb}})\}_{i,j=1}^k$ over R_0 . If the values of the partial derivatives $\frac{\partial g}{\partial x}$ and $\frac{\partial g}{\partial y}$ are not provided, estimate their values at the quadrature nodes via spectral partial differentiation:

$$\left[\frac{\partial g}{\partial x} \right] = \mathcal{D}_x^k[g] \quad \text{and} \quad \left[\frac{\partial g}{\partial y} \right] = \mathcal{D}_y^k[g]. \quad (214)$$

3. Compute an estimate

$$I_0 = \int_{R_0} f(x, y) \exp(ig(x, y)) dx dy \quad (215)$$

over the entire subrectangle using the subalgorithm described above.

4. Calculate estimates

$$I_i = \int_{R_i} f(x, y) \exp(i\omega \cdot g(x, y)) dx dy \quad (\text{For } i = 1, 2, 3, 4)$$

where

$$R_1 = \left[a_0, \frac{a_0 + b_0}{2} \right] \times \left[c_0, \frac{c_0 + d_0}{2} \right], \quad R_2 = \left[\frac{a_0 + b_0}{2}, b_0 \right] \times \left[c_0, \frac{c_0 + d_0}{2} \right], \quad (216)$$

$$R_3 = \left[a_0, \frac{a_0 + b_0}{2} \right] \times \left[\frac{c_0 + d_0}{2}, d_0 \right], \quad R_4 = \left[\frac{a_0 + b_0}{2}, b_0 \right] \times \left[\frac{c_0 + d_0}{2}, d_0 \right] \quad (217)$$

using the subalgorithm described above.

5. If $|I_0 - \sum_{i=1}^4 I_i| < \epsilon$, then update the current estimate $I \leftarrow I + I_0$. Otherwise, add $\{R_i\}_{i=1}^4$ to the stack of rectangles.

In the end, the algorithm returns the an estimate I for (5).

5.3 Adaptive Gauss-Legendre integration in 2D

In this section, we provide a brief description of the Gauss-Legendre adaptive integration scheme in two dimensions. In particular, we utilize this algorithm to compute accurate estimates of

$$\int_R f(x, y) dx dy \quad (218)$$

for some function $f : \mathbb{R}^2 \rightarrow \mathbb{R}$ and some rectangle $R \subset \mathbb{R}^2$. This algorithm was utilized in many of our experiments, and the values it returned were considered the ground truth.

Begin by constructing Legendre quadratures x_1, \dots, x_n and y_1, \dots, y_n on the intervals $[a, b]$ and $[c, d]$ respectively, along with associated Gauss-Legendre weights w_1^1, \dots, w_n^1 and w_1^2, \dots, w_n^2 . Taking a tensor product of the two sets of nodes yields a quadrature on the entire rectangle R , while taking pairwise products of the weights yields a set of

weights for the rectangle R . Explicitly, we obtain

$$\{x_i, y_j\}_{i,j=1}^n \quad \tilde{w}_{ij} = w_i^1 w_j^2 \quad (219)$$

The integral approximation of the function $f(x, y)$ over R is then given by

$$\int_R f(x, y) dx dy = \sum_{i,j=1}^n \tilde{w}_{ij} f(x_i, y_j) \quad (220)$$

The adaptive scheme takes as input an integer n denoting the order of the approximation, the values a, b, c, d denoting the bounds of integration, a tolerance parameter $\epsilon > 0$, and an external subroutine for evaluating the function $f(x, y)$ on the quadrature nodes. The algorithm maintains an approximation I which is initially set to 0, as well as a stack of subrectangles which initially contains the entire rectangle R . The following steps are repeated as long as the stack of rectangles is non-empty.

1. Remove a rectangle R_0 from the stack of rectangles.

2. Compute an estimate

$$I_0 = \int_{R_0} f(x, y) dx dy \quad (221)$$

over the entire subrectangle using the approximation (220) described above.

3. Compute estimates

$$I_i = \int_{R_i} f(x, y) dx dy \quad (\text{For } i = 1, 2, 3, 4.)$$

for the subrectangles R_i given by (217) used in the adaptive Levin algorithm.

4. If $\|I_0 - \sum_{i=1}^4 I_i\| < \epsilon$, then update the current estimate $I \leftarrow I + I_0$. Otherwise, add $\{R_i\}_{i=1}^4$ to the stack of rectangles.

When the algorithm terminates, an estimate I for (218).

6 Numerical Experiments

In this section, we provide the results of numerical experiments which were conducted to present the properties, behaviour, and performance of the two-dimensional adaptive Levin method in a variety of cases. The code for these experiments was written in Fortran, and compiled with version (blah).

We took $k = 7$, resulting in a 49 point tensor product quadrature on the unit rectangle built from a 7 point Clenshaw-Curtis quadrature. Moreover, we utilized $n_{\text{base}} = 9^{\text{th}}$ order bivariate Chebyshev expansions of the form Equation (27), resulting in 55 basis functions. Finally, we use a 7 point Curtis-Clenshaw rule when applying the one dimensional Levin method on each portion of the domain's boundary ∂R when applying the one dimensional Levin method. The tolerance parameter for the adaptive Levin method was set to 10^{-12} .

6.1 Integrals involving elementary functions with explicit solutions.

In this experiment, we evaluated the following integrals using the adaptive Levin scheme:

$$I_1(\omega) = \int_0^1 \int_{-100}^{100} \exp(i\omega(x+y)) dx dy, \quad (222)$$

$$I_2(\omega) = \int_{[-1,1]^2} \sin(x-y) \exp(i\omega(10x-4y)) dx dy \quad \text{and} \quad (223)$$

$$I_3(\omega) = \int_{[-1,1]^2} e^x \cos(y) \exp(i\omega(9y-2x)) dx dy. \quad (224)$$

These integrals have the following closed-form representations

$$I_1(\omega) = \frac{(e^{100i\omega} - e^{-100i\omega})(e^{i\omega} - 1)}{-\omega^2}, \quad (225)$$

$$I_2(\omega) = \frac{2i \sin(2\omega - 1) \sin(10\omega - 1)}{(4\omega - 1)(10\omega - 1)} - \frac{2i \sin(2\omega + 1) \sin(10\omega + 1)}{(4\omega + 1)(10\omega + 1)} \quad \text{and} \quad (226)$$

$$I_3(\omega) = \left(\frac{4\omega}{A} - \frac{2i}{A} \right) \sin(2\omega + i) (B \sin(C) + C \sin(B)), \quad (227)$$

where $A = BC(4\omega^2 + 1)$, $B = 9\omega + 1$ and $C = 9\omega - 1$.

In this experiment, we sampled $l = 200$ equispaced points x_1, \dots, x_l in the interval $[5, 20]$. For each $\omega = 2^{x_1}, \dots, 2^{x_l}$, we evaluated I_1, I_2 and I_3 using the adaptive Levin scheme. The time taken by the adaptive Levin scheme was measured and the absolute error on the solution was recorded. Figure 1 gives the results.

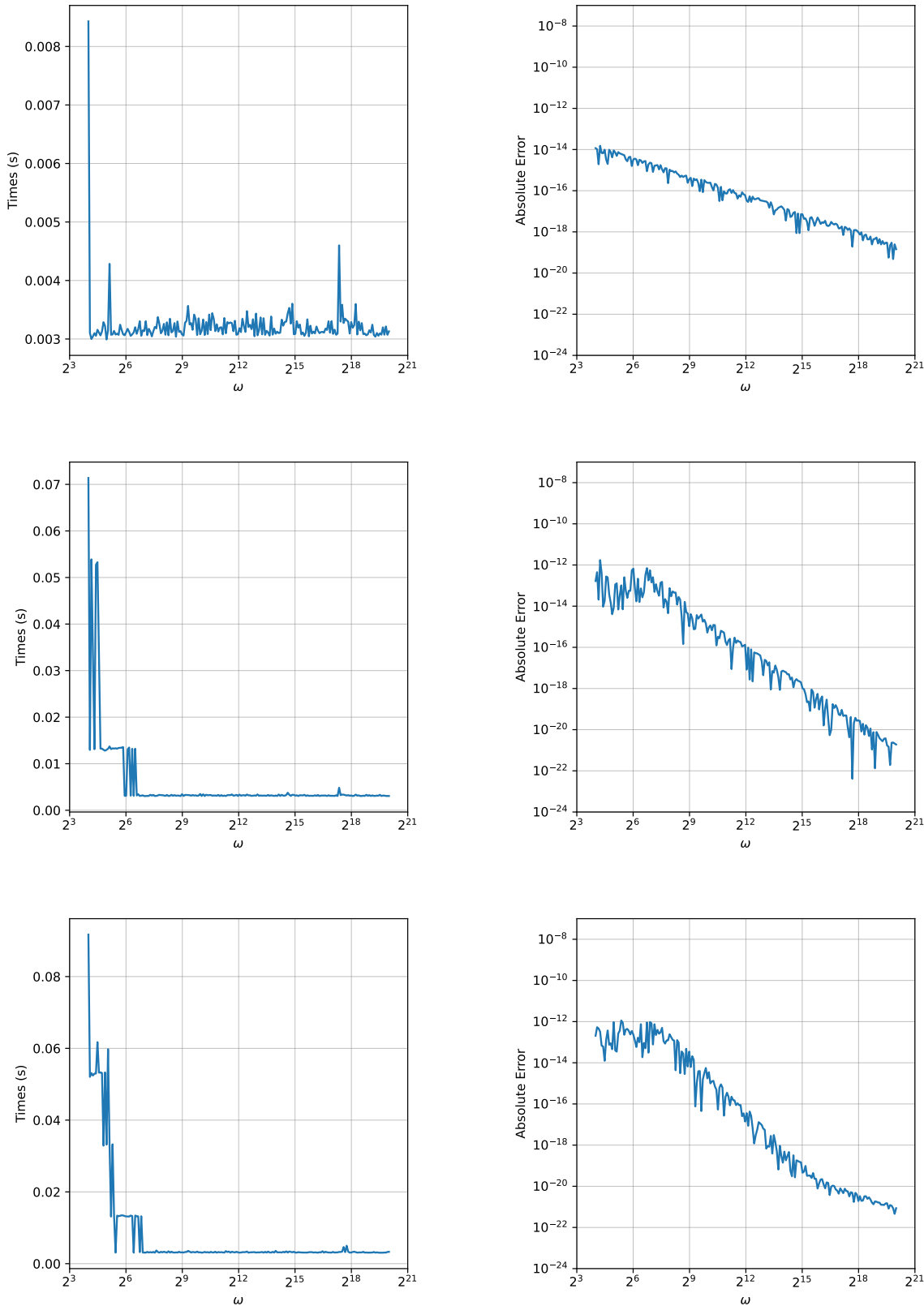


Figure 1: The results for the experiment in Section (6.1). The first row plots the results for integral I_1 over the rectangle $[0, 1] \times [-100, 100]$ in the case where $\omega = 2^{xi}$. The second and third rows plot the results for integrals I_2 and I_3 respectively in the case where $\omega = 2^i$. The plots in the first column display the computation time, which is notably independent of the frequency ω . The plots in the second column display the absolute error between the value computed by the two-dimensional adaptive Levin scheme and the true value provided by Equation (224).

6.2 Integrals with explicit solutions involving stationary points.

In this experiment, we evaluate

$$I_4(\omega) = \int_{[-1,1]^2} \exp(x+y) \exp(i\omega(x^2 - y^2)) dx dy \quad (228)$$

using the adaptive Levin scheme. This has a closed-form solution given by

$$I_4(\omega) = \frac{\pi}{4\omega} [\text{Erf}((-1)^{1/4}A) + \text{Erfi}((-1)^{1/4}B)] [\text{Erf}((-1)^{3/4}A) + \text{Erfi}((-1)^{3/4}B)] \quad (229)$$

$$(230)$$

where

$$A = \frac{1}{2\sqrt{\omega}} + i\sqrt{\omega} \quad B = \sqrt{\omega} + \frac{i}{2\sqrt{\omega}}. \quad (231)$$

The notation Erfi refers to the complex error function. This experiment was undertaken in order to understand the behaviour of the Levin method in the presence of stationary points. In this case, ∇g has stationary points along the lines $x = 0$ and $y = 0$.

We sampled $l = 200$ linearly-spaced points x_1, \dots, x_l in the interval $[5, 20]$, and we evaluated $I_4(\omega)$ for each $\omega = 2^{x_1}, \dots, 2^{x_l}$ using the adaptive Levin method. The computation times and absolute errors against the true solution are plotted in Figure 2 as a function of ω .

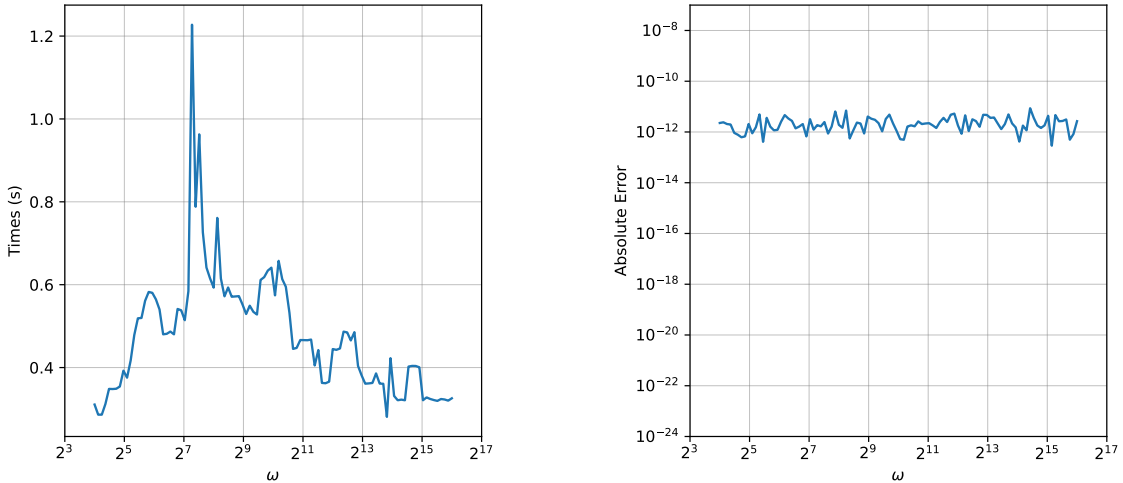


Figure 2: The results for the experiment in Section 6.2. The left and right plots provide the computation time and absolute error for integral I_4 and I_5 over the rectangle $[-1, 1]^2$ in the case where $\omega = (2^{x_i}, 2^{x_i})$ and $\omega = 2^{x_i}$ respectively.

6.3 An integral involving resonance points

In this experiment, we consider the integral

$$I_5(\omega) = \int_{[0,1]^2} \exp(i\omega(1+x)(1+y^2)) dx dy. \quad (232)$$

In this case,

$$\nabla g = \begin{pmatrix} 1+y^2 \\ 2y(1+x) \end{pmatrix}, \quad (233)$$

and so the integrand has a line of resonance points along $y = 0$. We sampled $l = 20$ linearly-spaced points x_1, \dots, x_l on the interval $[5, 20]$, and evaluated $I_5(\omega)$ for each $\omega = 2^{x_1}, \dots, 2^{x_l}$ using the adaptive Levin method. The computation times and relative errors, measured by comparison with the Gauss-Legendre adaptive scheme, are plotted in Figure 3 as a function of ω .

The relative errors are only computed up to $\omega = 2^{11}$ due to the time complexity in the case of the Gauss-Legendre method in the high frequency regime.

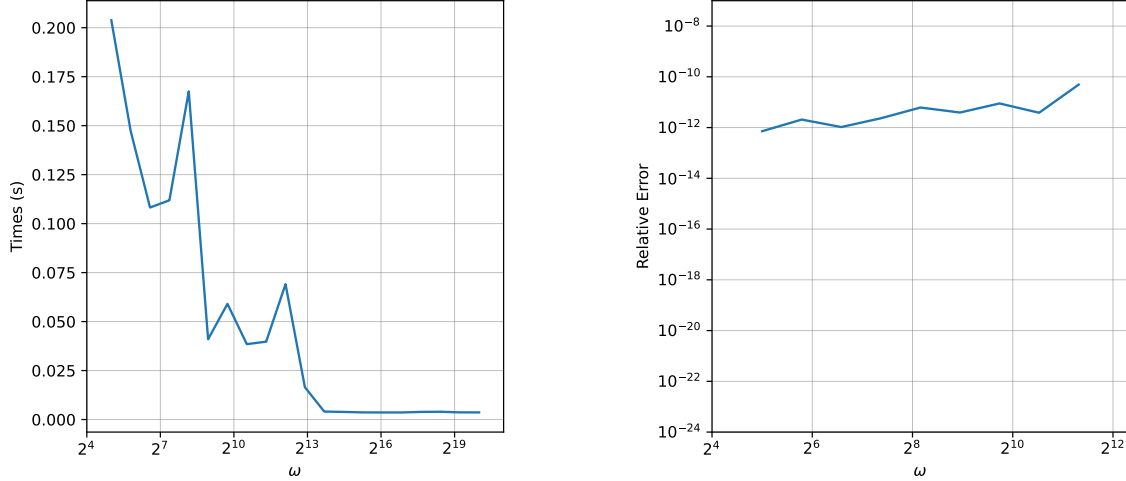


Figure 3: The results for the experiment in Section 6.2. The left and right plots provide the computation time and relative error for integral I_4 and I_5 over the rectangle $[-1, 1]^2$ in the case where $\omega = 2^{x_i}$. The relative error is obtained by direct comparison against the Gauss-Legendre adaptive integration scheme.

6.4 Integrals involving Bessel functions

In this experiment, we used the adaptive Levin method to evaluate the integral

$$I_6(\omega, \epsilon) = \int_{[0,1]^2 \setminus [0,\epsilon]^2} e^{x+y} H_0(\omega r) dx dy, \quad (234)$$

where

$$r = \sqrt{x^2 + y^2}. \quad (235)$$

Here, H_ν denotes the Hankel function of the first kind

$$H_\nu(x) = J_\nu(x) + iY_\nu(x), \quad (236)$$

where J_ν and Y_ν are Bessel functions of the first and second kind, respectively. They are solutions of Bessel's differential equation

$$x^2 \frac{d^2y}{dy^2}(x) + x \frac{dy}{dx}(x) + (x^2 - \nu^2)y(x) = 0. \quad (237)$$

The Bessel functions of the second kind are singular at the origin, making I_6 improper, which is why we delete a small neighbourhood of the origin from the domain of I_6 .

In this experiment, we sampled $l = 20$ equispaced points x_1, x_2, \dots, x_l on the interval $[5, 20]$. Then, for each $\omega = 2^{x_1}, \dots, 2^{x_l}$, we constructed a phase function representation for both the first and second kinds of Bessel functions using the algorithm of [2]. In particular, the phase α_ν^{bes} functions give us the representations

$$J_\nu(x) = \sqrt{\frac{\pi}{2x}} \frac{\sin(\alpha_\nu^{\text{bes}})}{\sqrt{\frac{d}{dx}\alpha_\nu^{\text{bes}}(x)}} \quad \text{and} \quad Y_\nu(x) = \sqrt{\frac{\pi}{2x}} \frac{\cos(\alpha_\nu^{\text{bes}})}{\sqrt{\frac{d}{dx}\alpha_\nu^{\text{bes}}(x)}}, \quad (238)$$

so that

$$H_\nu(x) = i \sqrt{\frac{\pi}{2x}} \frac{e^{-i\alpha_\nu^{\text{bes}}(x)}}{\sqrt{\alpha_\nu^{\text{bes}}(x)}}. \quad (239)$$

Using this representation, coupled with the adaptive Levin method, we evaluate I_6 . Explicitly, we took the following functions as input to the adaptive Levin scheme;

$$f(x, y) = i \sqrt{\frac{\pi}{2\sqrt{x^2 + y^2}}} \frac{e^{x+y}}{\sqrt{\alpha_0^{\text{bes}}(\omega\sqrt{x^2 + y^2})}} \quad \text{and} \quad (240)$$

$$g(x, y) = -\alpha_0^{\text{bes}}(\omega\sqrt{x^2 + y^2}) \quad (241)$$

The results of this experiment are plotted in Figure 4. Of course, the increased computation times for the calculation of I_6 in comparison to the other experiments can be attributed to the time taken to compute the vector of values $[\alpha_\nu^{\text{bes}}]$ at each iteration. Moreover, it is not surprising that as ϵ decreases in magnitude, a larger number of subdivisions are required in a neighbourhood of the singular. This is visually illustrated in the graph appearing on the right hand side of Figure 5, where we plot the subdivision pattern when we computed $I_6(2^{10}, \epsilon = 0.1)$.

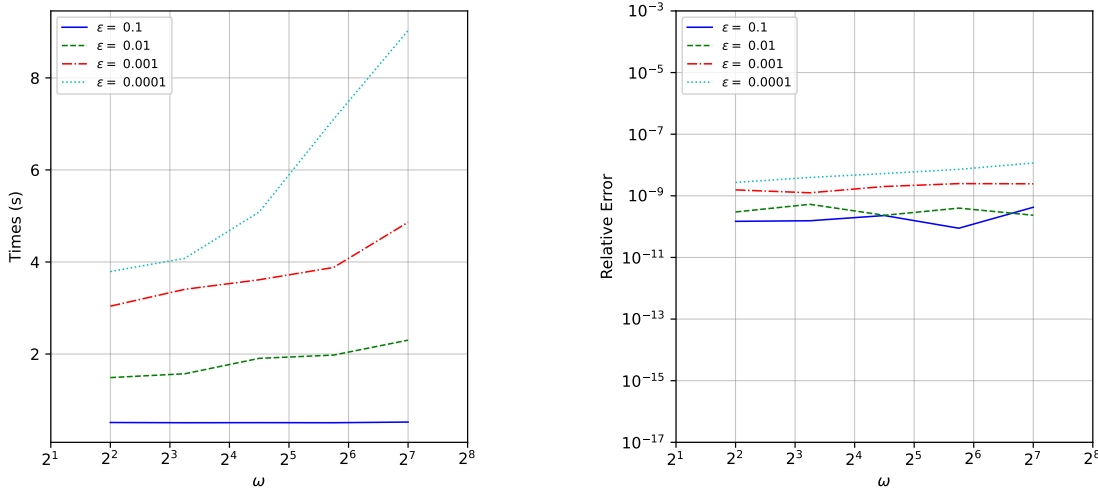


Figure 4: The results for the experiment in Section 6.4. The left and right plots provide the computation time and absolute error respectively a function of ω for integral I_6 over the rectangle $[0, 1]^2 \setminus [0, \epsilon]^2$ in the case where $\omega = 2^{x_i}$.

6.5 Experiment 5 - Behaviour in presence of high order stationary points

In this experiment, we used the adaptive Levin method to evaluate

$$I_7(\omega, n, m) = \int_{[-1,1]^2} \frac{\cos(xy)}{1+x^2+y^2} \exp(i\omega(x^n + y^m)) dx dy, \quad (242)$$

where n and m are positive integers. The goal of this experiment is to test the time-complexity of the algorithm as the order of the stationary points increases. The results of this experiment are shown in Figure 6. The first plots displays the computation time as a function of ω for each pair (n, m) while the second displays the relative error as a function of ω against the results for the adaptive Gauss-Legendre method. We consider the pairs

$$(n, m) = (2, 2), (3, 4), (4, 4) \text{ and } (7, 4). \quad (243)$$

Analogous to the results observed in [3], the relative error on the computed integral remains consistent for various pairs (n, m) , while the time complexity increases moderately with increasing $n + m$.

Displayed in Figure 7 are visualizations of the adaptive subdivision which occurred when the adaptive Levin method

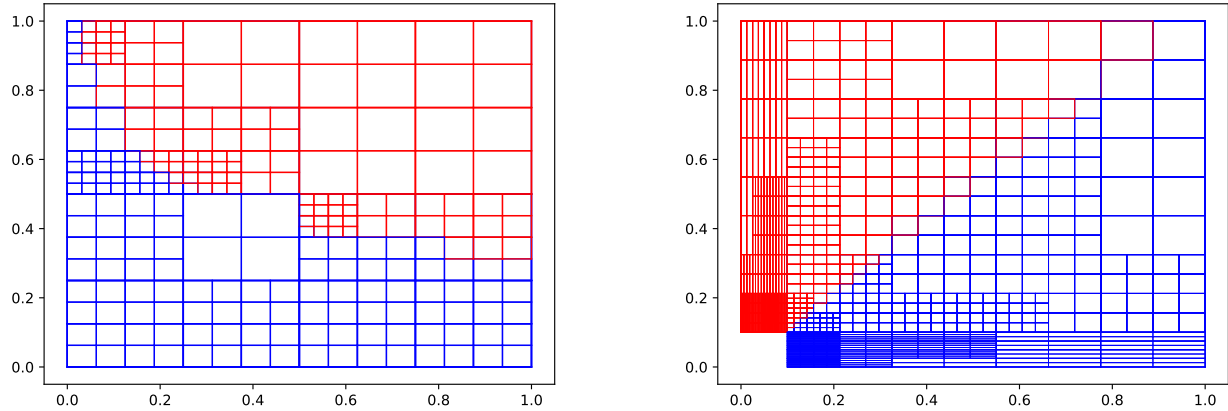


Figure 5: Plots visualizing the adaptive subdivision underwent by the two-dimensional adaptive Levin method. For a given subrectangle, the box boundary is colored blue if (205) was solved, and is colored red if (206) was solved. **(Left)** The subdivision when computing $I_4(\omega = 2^{10}, \epsilon = 0.1)$. **(Right)** The subdivision when computing $I_5(\omega = 2^{10}, \epsilon = 0.01)$.

was applied over the rectangular domain when computing $I_6(2^{12}, 2, 2)$ and $I_6(2^{12}, 2, 10)$.

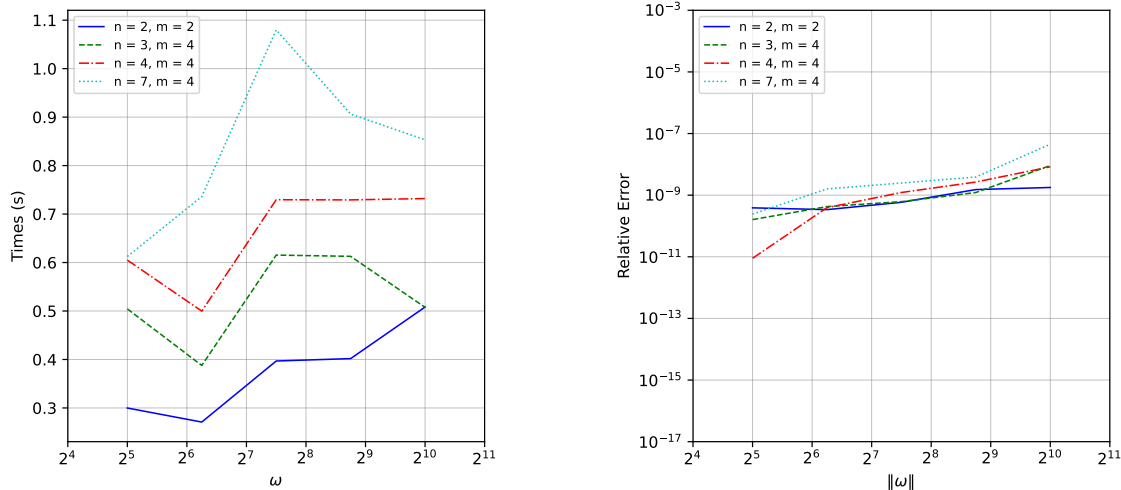


Figure 6: The results for the experiment in Section 6.5 where we analyze the behaviour of the adaptive Levin method in the presence of high-order stationary points. The left and right plots provide the computation time and absolute error respectively as a function of $|\omega|$ for integral $I_7(n, m)$. We consider various values of n and m over the rectangle $[-1, 1]^2$ and the case where $\omega = (2^{x_i}, 2^{x_i})$.

6.6 Experiment 6 - Behaviour in presence of many stationary points

In this experiment, we used the adaptive Levin method to evaluate

$$I_8(\omega, n, m) = \int_{[-1,1]^2} \frac{1}{1 + x^2 + y^2} \exp\left(i\omega \left(\sin^2\left(\frac{n\pi}{2}x\right) + \sin^2\left(\frac{m\pi}{2}y\right)\right)\right) dx dy \quad (244)$$

$$I_9(\omega, n, m) = \int_{[-1,1]^2} \frac{1}{1 + x^2 + y^2} \exp\left(i\omega \left(\sin^2\left(\frac{n\pi}{2}x\right) + \cos^2\left(\frac{m\pi}{2}y\right)\right)\right) dx dy \quad (245)$$

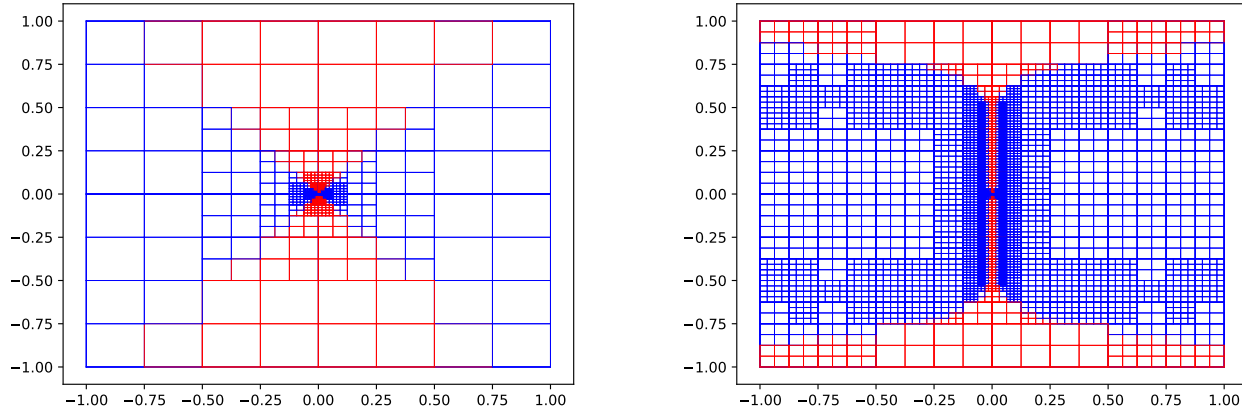


Figure 7: Plots visualizing the adaptive subdivision which occurred when the two-dimensional adaptive Levin method was applied. For a given subrectangle, the box boundary is colored blue if (205) was solved, and is colored red if (206) was solved. **(Left)** The subdivision when computing $I_6(\omega = 2^5, n = 2, m = 2)$. **(Right)** The subdivision when computing $I_7(\omega = 2^5, n = 2, m = 10)$.

each of which have nm stationary points, where n and m are positive integers. The goal of this experiment is to test the behaviour of the adaptive Levin method in the presence of many stationary points scattered across the domain of integration. In this experiment, we sampled $l = 30$ points x_1, \dots, x_l in the interval $[5, 20]$. Then, for each $\omega = (2^{x_1}, 2^{x_1}), \dots, (2^{x_1}, 2^{x_1})$, we evaluate I_8 for various values of (n, m) . We consider the pairs

$$(n, m) = (2, 2), (3, 4), (4, 4) \text{ and } (7, 4). \quad (246)$$

Figure 8 gives the results. Of course, it is not surprising to see that the time of computation increases uniformly as the number of stationary points increases. Additionally, Figure 9 provides a visualization of the adaptive subdivision underwent when computing $I_8(2^5, 3, 4)$ and $I_9(2^5, 4, 4)$.

7 Conclusion

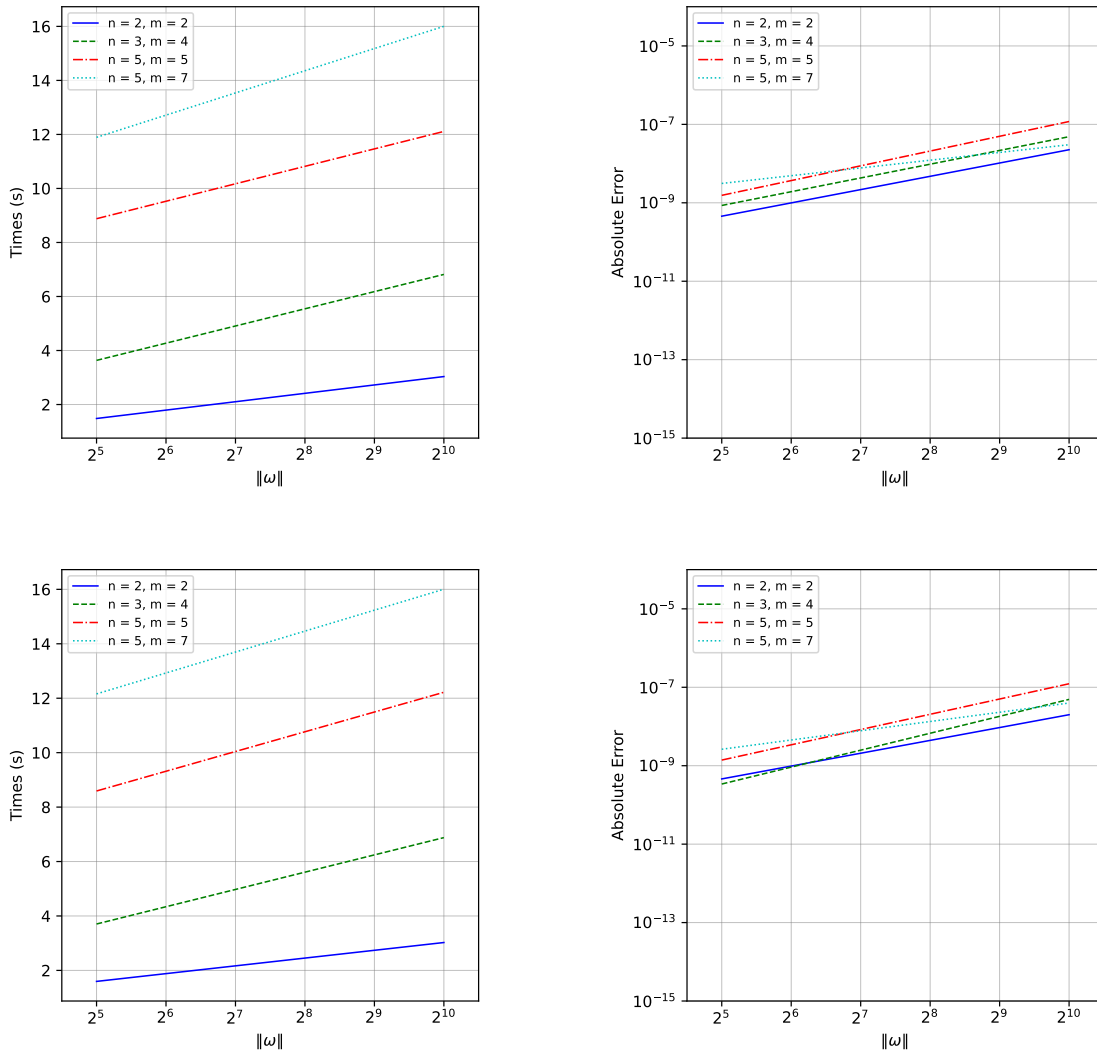


Figure 8: The results for the experiment in Section 6.6 where we analyze the behaviour of the adaptive Levin method in the presence of many stationary points. The left and right columns provide the computation time and absolute error respectively as a function of ω . The first row displays the results for $I_8(\omega, n, m)$ while the second column displays those of $I_9(\omega, n, m)$. We consider various values of n and m over the rectangle $[-1, 1]^2$ and the case where $\omega = (2^{x_i}, 2^{x_i})$.

References

- [1] John P. Boyd. “Approximation of an analytic function on a finite real interval by a bandlimited function and conjectures on properties of prolate spheroidal functions”. In: *Applied and Computational Harmonic Analysis* 15.2 (2003), pp. 168–176. ISSN: 1063-5203. DOI: [https://doi.org/10.1016/S1063-5203\(03\)00048-4](https://doi.org/10.1016/S1063-5203(03)00048-4). URL: <https://www.sciencedirect.com/science/article/pii/S1063520303000484>.
- [2] James Bremer. *Phase function methods for second order linear ordinary differential equations with turning points*. 2022. arXiv: 2209.14561.
- [3] Shukui Chen, Kirill Serkh, and James Bremer. *On the adaptive Levin method*. 2024. arXiv: 2211.13400 [math.NA].
- [4] David Levin. “Procedures for Computing One- and Two-Dimensional Integrals of Functions with Rapid Irregular Oscillations”. In: *Mathematics of Computation* 38.158 (1982), pp. 531–538. ISSN: 00255718, 10886842. URL: <http://www.jstor.org/stable/2007287> (visited on 05/17/2024).

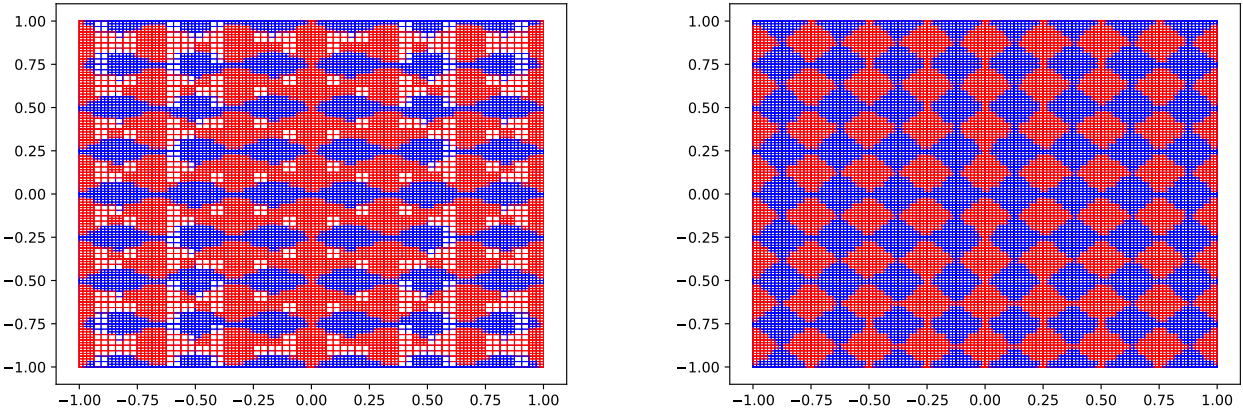


Figure 9: Plots visualizing the adaptive subdivision underwent by the two-dimensional adaptive Levin method. For a given subrectangle, the box boundary is colored blue if (205) was solved, and is colored red if (206) was solved. **(Left)** The subdivision when computing $I_8(\omega = 2^5, n = 3, m = 4)$. **(Right)** The subdivision when computing $I_9(\omega = 2^5, n = 4, m = 4)$.

- [5] Jianbing Li, Wang Xuesong, and Tao Wang. “A universal solution to one-dimensional oscillatory integrals”. In: *Science in China Series F: Information Sciences* 51 (Oct. 2008), pp. 1614–1622. DOI: [10.1007/s11432-008-0121-2](https://doi.org/10.1007/s11432-008-0121-2).
- [6] Jianbing Li et al. “An improved Levin quadrature method for highly oscillatory integrals”. In: *Applied Numerical Mathematics* 60.8 (2010), pp. 833–842. ISSN: 0168-9274. DOI: <https://doi.org/10.1016/j.apnum.2010.04.009>. URL: <https://www.sciencedirect.com/science/article/pii/S0168927410000735>.
- [7] Mohan Zhao and Kirill Serkh. *On the Approximation of Singular Functions by Series of Non-integer Powers*. 2023. arXiv: 2308.10439 [math.NA]. URL: <https://arxiv.org/abs/2308.10439>.